

Article

Discovery of 3-Ethyl-4-(3-isopropyl-4-(4-(1-methyl-1*H*-pyrazol-4-yl)-1*H*-imidazol-1-yl)-1*H*-pyrazolo[3,4-*b*]pyridin-1-yl)benzamide (TAS-116) as a Potent, Selective, and Orally Available HSP90 Inhibitor

Takao Uno, Yuichi Kawai, Satoshi Yamashita, Hiromi Oshiumi, Chihoko Yoshimura, Takashi Mizutani, Tatsuya Suzuki, Khoon Tee Chong, Kazuhiko Shigeno, Mitsuru Ohkubo, Yasuo Kodama, Hiromi Muraoka, Kaoru Funabashi, Koichi Takahashi, Shuichi Ohkubo, and Makoto Kitade

J. Med. Chem., **Just Accepted Manuscript** • DOI: 10.1021/acs.jmedchem.8b01085 • Publication Date (Web): 07 Dec 2018

Downloaded from <http://pubs.acs.org> on December 7, 2018

Just Accepted

"Just Accepted" manuscripts have been peer-reviewed and accepted for publication. They are posted online prior to technical editing, formatting for publication and author proofing. The American Chemical Society provides "Just Accepted" as a service to the research community to expedite the dissemination of scientific material as soon as possible after acceptance. "Just Accepted" manuscripts appear in full in PDF format accompanied by an HTML abstract. "Just Accepted" manuscripts have been fully peer reviewed, but should not be considered the official version of record. They are citable by the Digital Object Identifier (DOI®). "Just Accepted" is an optional service offered to authors. Therefore, the "Just Accepted" Web site may not include all articles that will be published in the journal. After a manuscript is technically edited and formatted, it will be removed from the "Just Accepted" Web site and published as an ASAP article. Note that technical editing may introduce minor changes to the manuscript text and/or graphics which could affect content, and all legal disclaimers and ethical guidelines that apply to the journal pertain. ACS cannot be held responsible for errors or consequences arising from the use of information contained in these "Just Accepted" manuscripts.



ACS Publications

is published by the American Chemical Society, 1155 Sixteenth Street N.W., Washington, DC 20036

Published by American Chemical Society. Copyright © American Chemical Society. However, no copyright claim is made to original U.S. Government works, or works produced by employees of any Commonwealth realm Crown government in the course of their duties.

Discovery of 3-Ethyl-4-(3-isopropyl-4-(4-(1-methyl-
1*H*-pyrazol-4-yl)-1*H*-imidazol-1-yl)-1*H*-
pyrazolo[3,4-*b*]pyridin-1-yl)benzamide (TAS-116)
as a Potent, Selective, and Orally Available HSP90
Inhibitor

Takao Uno,^{1} Yuichi Kawai,¹ Satoshi Yamashita,¹ Hiromi Oshiumi,² Chihoko Yoshimura,¹
Takashi Mizutani,¹ Tatsuya Suzuki,¹ Khoon Tee Chong,¹ Kazuhiko Shigeno,¹ Mitsuru Ohkubo,¹
Yasuo Kodama,¹ Hiromi Muraoka,¹ Kaoru Funabashi,¹ Koichi Takahashi,¹ Shuichi Ohkubo,¹
and Makoto Kitade³*

¹Discovery and Preclinical Research Division, Taiho Pharmaceutical Co. Ltd., Tsukuba, Ibaraki
300-2611, Japan

²Formulation Research, CMC Division, Taiho Pharmaceutical Co. Ltd., Kawauchi-cho,
Tokushima, Tokushima 771-0194, Japan

³Chemical Technology Laboratory, CMC Division, Taiho Pharmaceutical Co. Ltd., Kamikawa-
machi, Kodama-gun, Saitama 367-0241, Japan

Abstract

The molecular chaperone heat shock protein 90 (HSP90) is a promising target for cancer therapy, as it assists in the stabilization of cancer-related proteins, promoting cancer cell growth and survival. A novel series of HSP90 inhibitors were discovered by structure-activity relationship (SAR)-based optimization of an initial hit compound **11a** having a 4-(4-(quinolin-3-yl)-1*H*-indol-1-yl)benzamide structure. The pyrazolo[3,4-*b*]pyridine derivative, **16e** (TAS-116), is a selective inhibitor of HSP90 α and HSP90 β among the HSP90 family proteins and exhibits oral availability in mice. X-ray co-crystal structure of the **16e** analog **16d** demonstrated a unique binding mode at the *N*-terminal ATP binding site. Oral administration of **16e** demonstrated potent antitumor effects in an NCI-H1975 xenograft mouse model without significant body weight loss.

Introduction

Heat shock protein 90 (HSP90) is an adenosine triphosphate (ATP)-dependent molecular chaperone.^{1,2} ATP binds to the *N*-terminal of HSP90, and its hydrolysis facilitates folding of substrate proteins, referred to as HSP90 clients. Inhibition of HSP90 leads to the destabilization of HSP90 clients. HSP90 regulates more than two hundred HSP90 clients, including protein kinases, steroid hormone receptors, and transcription factors.²⁻⁴ Many of the HSP90 clients are oncoproteins that are involved in tumor development and survival. It is also known that HSP90 is over-expressed in cancer cells and tumor tissues, where it exists in a highly activated state.⁵⁻⁸ Therefore, HSP90 is considered to play a crucial role in cancer cell growth and survival. Based on these findings, ATP-competitive inhibitors acting at the *N*-terminal of HSP90 have been developed as therapeutic agents for cancer. Although some HSP90 inhibitors have shown clinical

1
2
3 efficacies, potential off-target and/or HSP90-related toxicities have proved problematic.^{3,4,9,10} For
4 instance, the first generation **1**¹¹(geldanamycin) analogs, such as **2**¹² (17-AAG), **3**¹³ (17-DMAG),
5 and their derivative **4**^{14,15} (IPI-504), have shown excess hepatotoxicity probably because of their
6 quinone structure.^{11,16,17} Although, small second-generation analogs with different structures
7 have shown low hepatotoxicity, some analogs such as purine-based derivative **5** (BIIB021)^{18,19}
8 exhibited neurological toxicities in a phase I trial.²⁰ In addition, visual disturbances have been
9 observed as an HSP90-related adverse event, although the frequency and degree varied among
10 the compounds.²¹ For instance, in a phase I trial of **7**²² (NVP-AUY922) derived from the natural
11 product **6**²³ (radicicol), 43% of patients experienced visual disturbances.²⁴ Further, clinical
12 development of **8**²⁵ (PF-04929113) was discontinued because of ocular toxicity observed in a
13 phase I study.²⁶ These results suggest that HSP90 inhibitors with different structures may exhibit
14 acceptable toxic profile with minimal off-target and HSP90-related toxicities. Alternatively, the
15 use of *C*- terminal inhibitor is another strategy to inhibit the HSP90 activity.³ The *C*-terminal
16 contains a nucleotide binding motif and mediates dimerization of HSP90.² It has been reported
17 that *N*-terminal HSP90 inhibitors induce a heat shock response (HSR) that is potentially involved
18 in drug resistance upon HSP90 inhibition.²⁷ During recent years, several *C*-terminal HSP90
19 inhibitors have been discovered. These inhibitors downregulate HSP90 clients and exhibit anti-
20 proliferative activity in several cancer cell lines without HSR.^{28,29} The clinical evaluation of
21 efficacy and toxicities of this class of compounds is the next challenge.

22
23
24 In this milieu, we aimed to develop a novel *N*-terminal HSP90 inhibitor that is different from
25 the known *N*-terminal inhibitors, such as **1**, **5**, **6**, and their derivatives, and with superior
26 druggability with respect to target selectivity and pharmacologic and pharmacokinetic profiles.

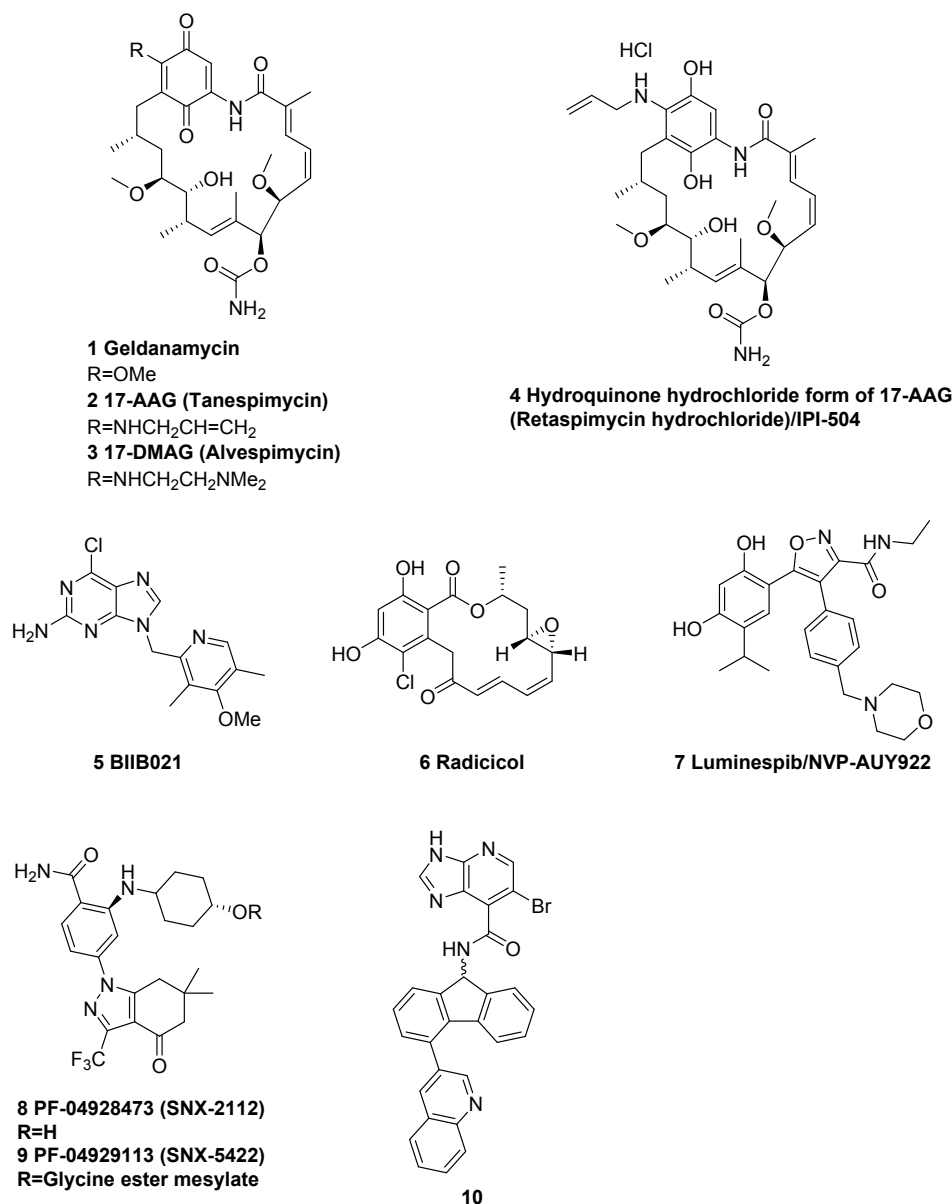


Figure 1. Structure of selected small molecular HSP90 inhibitors 1–10.

Results and Discussion

Drug design strategies. Several X-ray co-crystal structures of small molecular HSP90 inhibitors in complex with *N*-terminal ATP binding site of human HSP90 α have been reported.^{30,31} In this study, we designed a novel scaffold as HSP90 inhibitor using these X-ray co-crystal structures. Firstly, we investigated the X-ray co-crystal structure of the first and

second generation HSP90 inhibitors to analyze the binding mode to the HSP90 *N*-terminal ATP binding site.^{30,31} These binding modes have been commonly observed, forming a water-mediated hydrogen bond network with Asp93 and Thr184. Furthermore, the second generation HSP90 inhibitor **8** analogs^{25,32,33} form hydrogen bonds with Tyr 139 and Lys 58 in addition to the above two common hydrogen bonds. Secondly, we focused on the structures of **8**^{25,32} and **10**,³⁴ which are different from natural products, such as **1** and **6** analogs, and purine analogs such as **5**. However, the X-ray co-crystal structures of **8** and **10**, neither with each other nor with HSP90 individually, have been reported. Therefore, we speculated the binding mode of **8** and **10** based on the previously reported X-ray co-crystal structure of **8** analogs (PDB entry: 3DOB, 3MNR)^{25,32,33} and made a superposition of **8** and **10** (Figure 2A). Figure 2A shows the simplified scheme including four key hydrogen bonds of **8** and **10** with the HSP90 *N*-terminal ATP binding site. The speculated binding mode common to **8** and **10** are as follows. (i) The carboxamide group of **8** and pyrrolopyridine group of **10** act as adenine mimics with the amide group forming hydrogen bonds with Asp93 and Thr184. (ii) The hydroxyl group of *trans*-4-hydroxycyclohexylamino moiety forms hydrogen bonds with Lys58. (iii) The carbonyl group of **8** and nitrogen atom of 3-quinoline group of **10** form a hydrogen bond with Tyr139. Through the superposition of the speculated binding mode of compounds **8** and **10**, we designed a hybrid compound **11a** by combining these key hydrogen bonds (Figure 2B). The hybrid compound **11a** exhibited moderate HSP90 binding inhibitory activity ($IC_{50} = 9.5 \mu M$). The result encouraged us to develop a novel HSP90 inhibitor. Subsequently, this compound was also reported by Mailliet et al.³⁵ Therefore, we devised two drug design strategies aiming to further enhance the HSP90 binding inhibitory activity, as shown in Figure 2C. Strategy 1 involved the introduction of a substituent to fill the small hydrophobic pocket and the introduction of nitrogen atom into the

indole core. This strategy was supported by a previous study by Huang et al.,²⁵ which reported that the filling of small hydrophobic pocket contributed significantly to the HSP90 binding inhibitory activity. Strategy 2 involved exploration of an alternative structure of 3-quinoline group based on the SAR study.

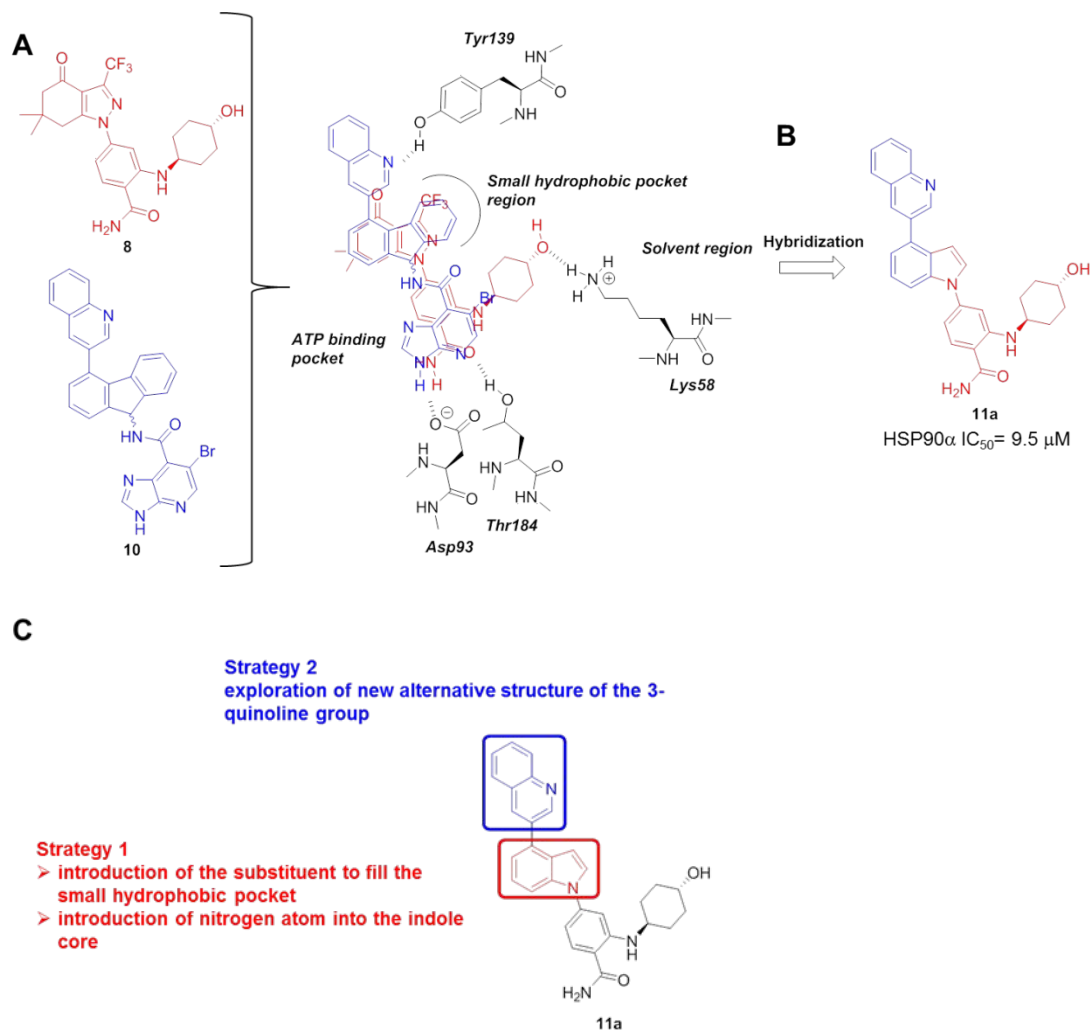
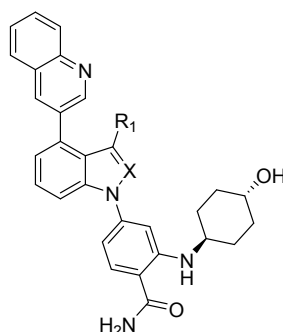


Figure 2. (A) Superposition of the speculated binding mode of **8** and **10**, a hybridization strategy used to design novel HSP90 inhibitors. (B) The structure and HSP90 binding inhibitory activity of 4-(1*H*-indol-1-yl)benzamide hit **11a**. (C) Drug design strategies to enhance the HSP90 binding inhibitory activity.

Strategy 1: Structure-activity relationship exploration of the indole core in the initial hit

11a. As mentioned above, the introduction of an alkyl chain at the C-3 position of the indole ring in **11a** with the intent to fill the small hydrophobic pocket formed by the residues Ala111, Val138, and Tyr139 is likely to enhance the HSP90 binding inhibitory activity. To confirm this hypothesis, we designed compound **11b**, in which the C-3 position of the indole ring in **11a** was substituted with a methyl group. In addition, we also designed compound **12a**, in which a nitrogen atom was introduced into the indole ring of **11a**. Table 1 shows the HSP90 inhibitory activity of **11a** and **12a**, determined based on the binding of HSP90 by the alphascreen competitive assay. The HSP90 binding inhibitory activity of **11b** was significantly enhanced by the introduction of a methyl group at the C-3 position of the indole ring. In addition, the indazole derivative **12a**, which is an *N*-inserted derivative of **11a**, also exhibited good HSP90 binding inhibitory activity. Based on these results, we aimed to further enhance the HSP90 binding inhibitory activity and investigated the effect of introduction of various alkyl chains at the C-3 position in the indazole derivative **12a**. Most alkyl-substituted indazole derivatives showed good HSP90 binding inhibitory activity with IC₅₀ values less than 100 nM. Among them, **12c** with an isopropyl group at the C-3 position in **12a** presented the highest affinity toward HSP90. Based on its potent HSP90 binding inhibitory activity, we selected the 3-isopropyl derivative **12c** as the hit compound for further optimization.

Table 1. Biological data of compounds with 3-alkyl and nitrogen substitution at the indole core



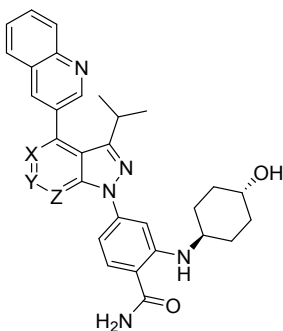
Compd	X	R ₁	HSP90 α IC ₅₀ (nM) ^a
11a	CH	H	9524 \pm 4870
11b	CH	Me	585 \pm 85
12a	N	H	365 \pm 64
12b	N	Me	94 \pm 13
12c	N	<i>i</i> -Pr	67 \pm 16

^aThe interaction of compounds with HSP90 was determined by the alphascreen competitive assay. The IC₅₀ values (nM) are shown as mean \pm SE (n = 3).

At this point of the study, the 3-isopropyl derivative **12c** represented the most advanced analog and demonstrated potent HSP90 binding inhibitory and tumor cell growth inhibitory activities in SK-BR-3 cells (HER2-overexpressing human breast cancer cell line); however, it evidently exhibited hERG inhibitory activity (Table 2). Therefore, with the aim to lower the hERG inhibitory activity of **12c**, we examined the reduction in lipophilicity by introducing a nitrogen atom into the indazole ring. Table 2 shows the HSP90 binding inhibitory and tumor cell growth inhibitory activities of **12c** in SK-BR-3 cells, as well as its *in vitro* hERG inhibitory activity. Compound **13a**, in which a nitrogen atom was inserted at the X position of indazole in **12c**, showed highly attenuated HSP90 binding and cellular activities in SK-BR-3 cells compared with those of **12c**. In addition, compound **13b**, in which a nitrogen atom was inserted at the Y position, did not exhibit lowered lipophilicity and hERG inhibition. Furthermore, **13b** also

exhibited significantly attenuated cellular activity in SK-BR-3 cells. On the contrary, compound **13c**, in which a nitrogen atom was inserted at the Z position, showed equally potent HSP90 binding inhibitory and cellular activities in SK-BR-3 cells when compared with those of **12c**. In addition, the pyrazolo[3,4-*b*]pyridine derivative **13c** showed lower hERG inhibitory activity than that of indazole **12c**. Further, nitrogen substitution at the Z position lowered the LogD value of the resulting pyrazolo[3,4-*b*]pyridine analog. Based on these results, we decided to perform SAR study of the pyrazolo[3,4-*b*]pyridine **13c**.

Table 2. Biological data of compounds with nitrogen substitution at the indazole core



Compd	X	Y	Z	HSP90α IC ₅₀ (nM) ^a	SK-BR-3 IC ₅₀ (nM) ^b	LogD ^c	hERG %Inhibition (at 10 μM) ^d
12c	CH	CH	CH	67±16	39±10	3.9±0.3	60±3
13a	N	CH	CH	470±55	1721±351	3.3±0.1	35±2
13b	CH	N	CH	72±10	473±430	4.0±0.2	57±4
13c	CH	CH	N	58±3	54±16	3.4±0.1	37±3

^aThe interaction of compounds with HSP90 was determined by the alphascree competitive assay. The IC₅₀ values (nM) are shown as mean ± SE (n = 3).

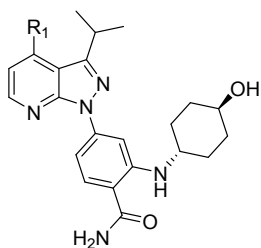
^bSK-BR-3 cells were cultured with the compounds for 72 h. Cell survival was then measured and the IC₅₀ value was calculated. The IC₅₀ values (nM) are shown as mean ± SE (n = 3).

^cLogD value at pH 7.4.³⁶ The LogD values (nM) are represented as mean ± SD (n = 3).

^dThe hERG inhibitory activity of compounds at a concentration of 10 μ M. The values of hERG percent inhibition are shown as mean \pm SE (n = 3).

Strategy 2: Structure-activity relationship exploration of an alternative structure of the 3-quinoline group. To further enhance the HSP90 binding and cellular activities, we examined the effect of introduction of other C-4 substituents in place of 3-quinoline group. Table 3 shows the HSP90 binding inhibitory and growth inhibitory activities in SK-BR-3 cells. Naphthalene **14a** and phenyl **14b**, in which the nitrogen atom at the N-3 position of the 3-quinoline group was removed, significantly decreased the HSP90 binding and cellular activities. The results suggested that the nitrogen atom in the 3-quinoline group is essential for the formation of hydrogen bond with Tyr139, similar to that of our speculated binding mode (Figure 2A). Therefore, we examined the effect of introduction of various substituted pyridine groups. 3-Pyridine **14c** and its 6- and 5-methoxy substituted derivatives **14d** and **14e**, and other bicyclic 3-pyridine derivatives **14f** and **14g**, other than the 3-quinoline group, tended to exhibit reduced potencies against HSP90 binding and tumor cell growth. On the contrary, thiophene **14h** and furan **14i** with sulfur and oxygen atoms at the C-4 position, respectively, did not exhibit measurable HSP90 binding and cellular activities. In contrast, imidazole **15a** showed marginally higher inhibitory activity against HSP90 binding than that by **14h** and **14i**. In addition, compound **15b** with a phenyl group at the C-4 position of imidazole showed significantly enhanced inhibitory activity against HSP90 binding and tumor cell growth. Based on these findings, the 4-phenylimidazole derivative **15b** was selected for further optimization as a candidate with an alternative structure of the 3-quinoline group.

Table 3. Preliminary structure and biological data of 3-quinoline derivatives



Compd	R ₁	HSP90α IC ₅₀ (nM) ^a	SK-BR-3 IC ₅₀ (nM) ^b	Compd	R ₁	HSP90α IC ₅₀ (nM) ^a	SK-BR-3 IC ₅₀ (nM) ^b
13c		58±3	54±16	14f		789±132	1132±272
14a		>10000	>10000	14g		750±123	423±105
14b		>10000	>10000	14h		>10000	>10000
14c		166±6	464±69	14i		>10000	>10000
14d		1168±87	1358±228	15a		1620±386	7300±981
14e		183±29	451±110	15b		132±24	276±81

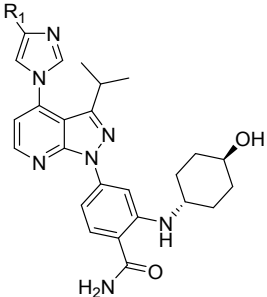
^aThe interaction of compounds with HSP90 was determined by the alphascreen competitive assay. The IC₅₀ values (nM) are shown as mean ± SE (n = 3).

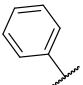
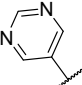
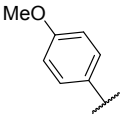
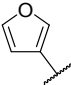
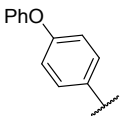
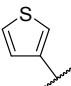
^bSK-BR-3 cells were cultured with the compounds for 72 h. Cell survival was then measured and the IC₅₀ value was calculated. The IC₅₀ values (nM) are shown as mean ± SE (n = 3).

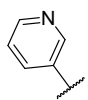
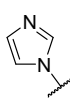
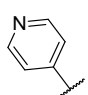
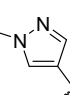
Exploration of an alternative structure of the 3-quinoline group. To further enhance the HSP90 binding inhibitory and growth inhibitory activities in SK-BR-3 cells, we examined the effect of introduction of other C-4 substituents in place of the phenyl group in **15b**. Table 4

shows HSP90 binding inhibitory and growth inhibitory activities in SK-BR-3 cells. The 4-methoxy phenyl derivative **15c** retained the HSP90 binding and cellular activities, but the 4-phenoxyphenyl derivative **15d** showed reduced potencies against HSP90 binding and tumor cell growth. Various heterocyclic derivatives **15e-k** have a tendency to increase the inhibitory activity against HSP90 binding and tumor cell growth. Among them, compound **15k** with a methyl pyrazole group showed the most potent growth inhibitory activity in SK-BR-3 cells. Furthermore, **15k** showed more potent inhibitory activity against HSP90 binding and tumor cell growth than those of the 3-quinoline derivative **13c**. With Strategies 1 and 2, we succeeded in identifying the most potent methyl pyrazole derivative **15k**.

Table 4. Biological data of compounds with 4-substitution at the imidazole ring



Compd	R ₁	HSP90α IC ₅₀ (nM) ^a	SK-BR-3 IC ₅₀ (nM) ^b	Compd	R ₁	HSP90α IC ₅₀ (nM) ^a	SK-BR-3 IC ₅₀ (nM) ^b
15b		132±24	276±81	15g		91±14	387±19
15c		96±15	256±8	15h		73±8	146±7
15d		643±119	503±80	15i		87±15	145±23

15e		48±8	41±20	15j		52±9	103±16
15f		55±7	165±26	15k		54±10	36±6

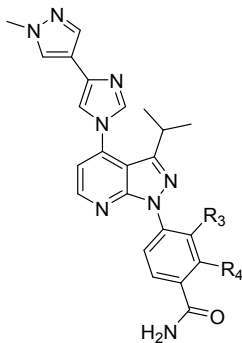
^aThe interaction of compounds with HSP90 was determined by the alphascreen competitive assay. The IC₅₀ values (nM) are shown as mean ± SE (n = 3).

^bSK-BR-3 cells were cultured with the compounds for 72 h. Cell survival was then measured and the IC₅₀ value was calculated. The IC₅₀ values (nM) are shown as mean ± SE (n = 3).

Optimization of the benzamide group. At this point of the study, the methyl pyrazole derivative **15k** represented the most advanced analog and demonstrated potent inhibitory activity against HSP90 binding and tumor cell growth. However, compound **15k** did not exhibit measurable oral exposure in mice (Table 5), although it had good metabolic stability (data not shown). This suggested that the low oral exposure in mice might be attributed to the large molecular weight (MW) and topological polar surface area (TPSA), high LogD value, and low solubility at neutral pH (pH 7.4). Therefore, to improve its oral exposure in mice, we examined the optimization of benzamide substituents in order to reduce MW, TPSA, and LogD value, and to improve solubility at pH 7.4. Table 5 shows the HSP90 binding inhibitory and growth inhibitory activities in SK-BR-3 cells, and also their MW, TPSA, LogD, solubility at pH 7.4, and oral exposure in mice (AUC_{0-6h} (μM*h)). Although the cellular activity of compound **16a**, without the 4-aminocyclohexanol group, was highly attenuated, it showed a certain level of oral exposure in mice. The result suggested that the reduction in MW, TPSA, and LogD value of **16a** might be important for improving oral exposure. Compound **16b**, having a 4-aminomethyl group with minimized 4-aminocyclohexanol structure, showed attenuated cellular activity when compared with that of **15k**. On the contrary, **16c** having a 3-aminomethyl group at R₃ position showed HSP90 binding inhibitory activity similar to that of **15k**, and the cellular activity also

increased when compared with that of **16a** and **16b**. Furthermore, by shifting the substitution position from C-4 to C-3, the LogD value of **16c** decreased significantly. In addition, the oral exposure of **16c** in mice was similar to that of compound **16a**. Based these results, we successfully acquired a favorable derivative with oral exposure in mice by minimizing the 4-aminocyclohexanol group, thus reducing the MW, TPSA, and LogD value. In addition, these results suggested that the position of substitution is better in R₃ than in R₄. To further improve their oral exposure in mice, we examined the introduction of other R₃ substituents in place of 3-aminomethyl group. Compound **16d**, in which the aminomethyl group was converted to methyl group as the smallest alkyl group, with reduced TPSA and increased LogD value, showed attenuated inhibitory activity against HSP90 binding and tumor cell growth when compared with those of **16c**. In contrast, the solubility of **16d** at pH 7.4 was highly improved and its oral exposure in mice was also highly improved when compared with those of **16c**. Compound **16e** with ethyl group showed increased inhibitory activity against HSP90 binding and tumor cell growth. In particular, the oral exposure of **16e** in mice was further improved when compared with that of **16d**. Based on these results, we succeeded in obtaining **16e** with favorable oral exposure in mice by optimizing the balance of MW, TPSA, LogD value of **15k**, and improving the solubility of **15k** at pH 7.4. These results suggest that the 4-aminocyclohexanol group in the methylpyrazole derivative **15k** has negligible effect against the HSP90 binding inhibitory activity when compared with that of **16e**. That is, it suggests that the contribution of interactions, which might be formed by the 4-(1*H*-imidazol-4-yl)-1-methyl-1*H*-pyrazole and 3-ethylbenzamide groups of **16e**, is more important for the HSP90 binding inhibitory activity. In addition, these results also suggest that the solubility at pH 7.4 greatly affects oral exposure in mice.

Table 5. Biological data of compounds with substitution at the benzamide ring



Compd	R ₃	R ₄	MW	TPSA	LogD ^a	Solubility pH 7.4 (μM) ^b	HSP90α IC ₅₀ (nM) ^c	SK-BR-3 IC ₅₀ (nM) ^d	AUC _{0-6h} (μM*h) ^e
15k	-H		539.64	134.51	3.6±0.2	3±1	54±10	36±6	N.D. ^f
16a	-H	-H	426.48	102.25	3.0±0.3	4±1	204±14	1636±323	5.00
16b	-H	-NHMe	455.53	114.28	3.0±0.3	<2	131±37	773±129	N.T. ^g
16c	-NHMe	-H	455.53	114.28	1.9±0.2	15±2	58±6	419±105	2.69
16d	-Me	-H	440.51	102.25	2.1±0.2	>170	98±10	1137±336	37.69
16e	-Et	-H	454.54	102.25	2.4±0.2	>170	69±11	330±119	90.1

^aLogD value at pH 7.4.³⁶ The LogD values (nM) are shown as mean ± SD (n = 3).

^bSolubility at pH 7.4.³⁷ Solubility (μM) is shown as mean ± SD (n = 3).

^cThe interaction of compounds with HSP90 was determined by the alphascreen competitive assay. The IC₅₀ values (nM) are shown as mean ± SE (n = 3).

^dSK-BR-3 cells were cultured with the compounds for 72 h. Cell survival was then measured and the IC₅₀ value was calculated. The IC₅₀ values (nM) are shown as mean ± SE (n = 3).

^eBalb/cA male mice (n = 2) were orally administered at a dose of 50 mg/kg.

^fNot detected at all time points (lower limit of quantification = 0.03 μM).

^gNot tested.

Structural analysis and discussion of compound 16d. To rationalize the structural basis for the potent HSP90 binding affinity of 3-ethyl-4-(3-isopropyl-4-(4-(1-methyl-1*H*-pyrazol-4-yl)-1*H*-imidazol-1-yl)-1*H*-pyrazolo[3,4-*b*]pyridin-1-yl)benzamide **16e**,³⁸ we tried to acquire its X-ray co-crystal structure in complex with *N*-terminal ATP binding site of human HSP90α. However, we were unable to obtain it. Therefore, we determined the X-ray co-crystal structure of **16d** as **16e** (TAS-116) analog in complex with *N*-terminal ATP binding site of human HSP90α (Figure 3). As expected, the carboxamide group behaved as an adenine mimic and formed a water-mediated hydrogen bond network with Asp93 and Thr184. The phenyl group is sandwiched between Met98 and Asn51. This suggests that the alkyl group in the benzamide ring at C-3 position might lead to appropriate twist conformation against pyrazolo[3,4-*b*]pyridine ring. The pyrazolo[3,4-*b*]pyridine core occupies a hydrophobic region formed by Leu107, Phe138, and Trp162. In addition, the isopropyl group at the C-3 position in the pyrazolo[3,4-*b*]pyridine core fills the small hydrophobic pocket formed by Ala111, Tyr139, and Val136. This helical specific pocket formed by the rearrangement of Ile110-Gly114 residues has also been previously observed in other HSP90 inhibitors.^{30,39} Furthermore, the nitrogen atom at the N-2 position of pyrazolo[3,4-*b*]pyridine forms a water-mediated hydrogen bond network with Asn51. As expected, the nitrogen atom at the N-3 position of the imidazole group at the C-4 position of pyrazolo[3,4-*b*]pyridine forms a hydrogen bond with Tyr139. Moreover, the methylpyrazole

group introduced at the imidazole C-4 position occupies a hydrophobic subpocket with Phe22, Ile26, Ile104, Gly108, and Phe170 (Figure 3B). These results suggest that the enhancement of HSP90 binding inhibitory activity and the binding mode of **16d** observed by X-ray co-crystal structure analysis are correlated. Based on these results, the **16e** (TAS-116) analog **16d** was considered to have a unique binding mode that has not been observed in the typical first and second generation HSP90 inhibitors.³⁰ The hydrogen bond with Tyr139 and water-mediated hydrogen bond network with Gln23 were observed in other HSP90 inhibitors by Vallée et al.⁴⁰

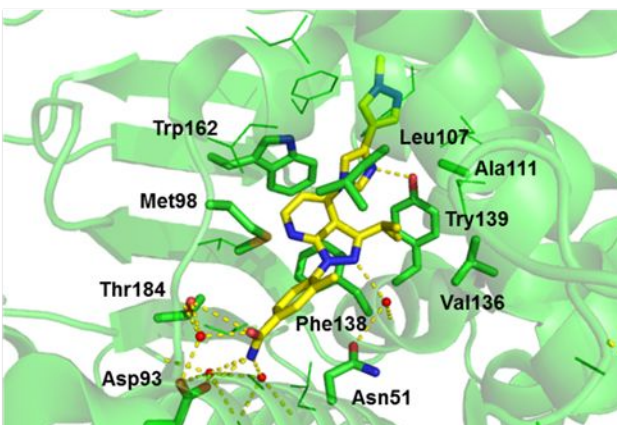
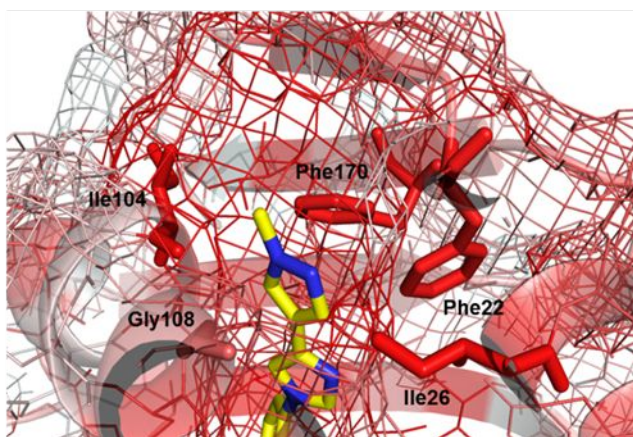
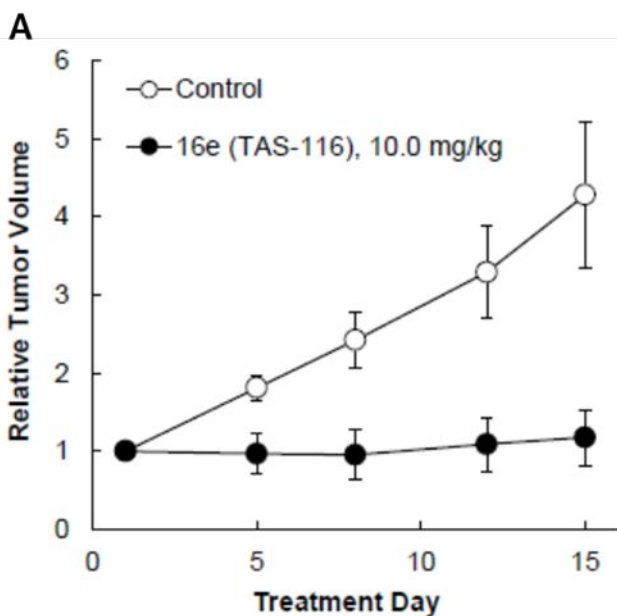
A**B**

Figure 3. (A) Co-crystal structure of compound **16d** bound to the *N*-terminal ATP binding site of human HSP90. (B) The molecular surface representation of the co-crystal structure of compound **16d** in hydrophobic (red) to non-hydrophobic (white) gradient (PDB:5ZR3).

Based on its promising HSP90 inhibitory activity and oral availability profile, the *in vitro* profile and pharmacokinetic (PK) properties of compound **16e** was characterized.⁴¹ Compound **16e** selectively binds to HSP90 α/β than to the highly homologous HSP90 family proteins GRP94 and TRAP1, as determined by the fluorescence polarization competitive binding assay with geldanamycin-FITC.^{42,43} In addition, **16e** did not inhibit other ATPases, such as HSP70 and HSP48, among different protein kinases tested. Regarding the toxicity of **16e** toward non-cancer cell lines, the IC₅₀ value of normal human stromal cells was more than 5 μ M.⁴⁴ Furthermore, **16e** demonstrated good metabolic stability in isolated hepatocytes of rodent and non-rodent species (data not shown). Moreover, **16e** did not inhibit the major human cytochrome P450 enzyme *in vitro* at *in vivo* effective concentrations of **16e**. It also showed good bioavailability in rodent and non-rodent species. Further, **16e** was distributed less in the eye tissues than in the plasma of rats; consequently, **16e** did not cause any detectable ocular toxicity, while **7** induced photoreceptor cell death in rats.⁴¹ These results suggest that the novel orally available HSP90 α/β selective inhibitor **16e** has a favorable profile as a potential clinical candidate.

***In vivo* pharmacology of 16e.** Based on the favorable *in vitro* profiles and PK properties, compound **16e** was further evaluated in a human tumor xenograft model. Shown in Figure 4A is the *in vivo* antitumor activity of **16e** in an NCI-H1975 (EGFR L858R/T790M)⁴⁵ xenograft model of mice, and the mean body weight change (BWC) (%) is shown in Figure 4B. Reflecting its potent HSP90 inhibitory activity, compound **16e** exhibited potent efficacy (tumor/control ratio

[T/C]: 27%) after the daily oral administration of **16e** for 14 days at a dose of 10 mg/kg without significant body weight loss in mice. The level of tumor proteins at 12 h after the last administration of **16e** for 3 days at a dose of 10.0 mg/kg, determined by western blot analysis, is shown in Figure 4C. Compound **16e** induced a marked decrease in the level of EGFR, thus, inhibiting downstream signaling, such as phospho-AKT, phospho-RPS6, and phospho-MAPK1/3. These results suggest that **16e** has antitumor effects in an EGFR-driven tumor model. In addition, these results suggested that **16e** demonstrates its antitumor effects by decreasing the level of mutant EGFR, thereby, inhibiting the mutant EGFR-activated AKT and MAPK 1/3 signaling pathways, which are involved in the survival and proliferation of tumors. Therefore, **16e** might be used to develop an effective chemotherapy for HSP90 client-driven cancer such as lung cancer-expressing mutant EGFR.



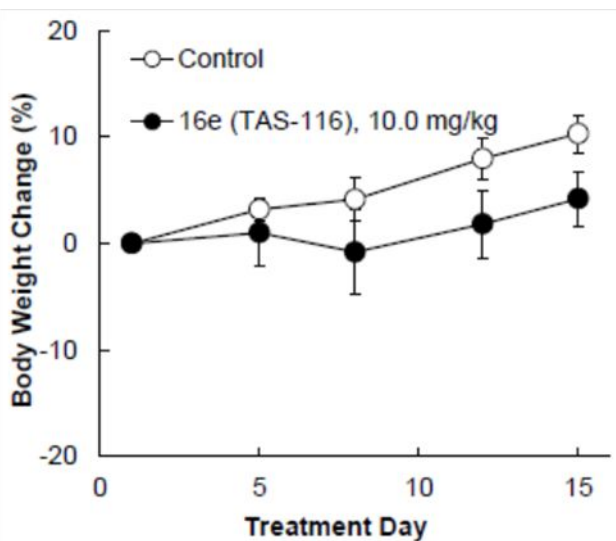
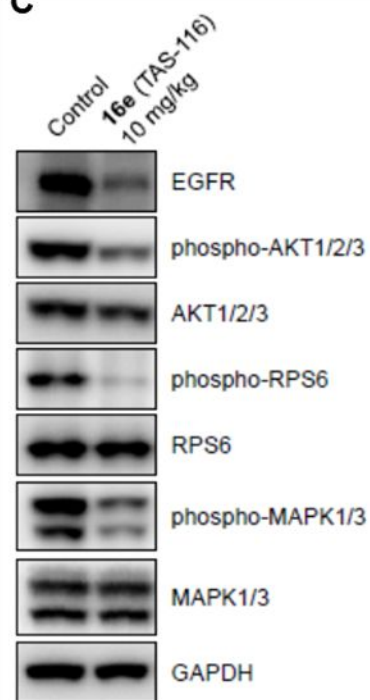
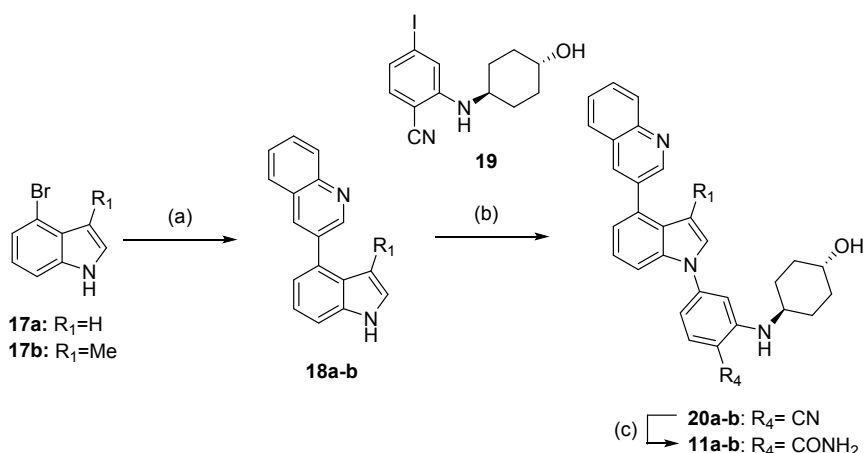
B**C**

Figure 4. (A) Antitumor efficacy of **16e** (TAS-116) in athymic nude mice bearing NCI-H1975 human lung cancer xenografts. (B) Body weight change of the tumor-bearing mice administered **16e** (TAS-116). (C) Pharmacodynamic activity of **16e** (TAS-116) in the NCI-H1975 tumors.

Chemistry

The initial hit compound **11a** and 3-substitued indole derivative **11b** were synthesized by the method shown in Scheme 1. Commercially available 4-bromoindole **17a-b** were reacted with 3-quinolineboronic acid under Suzuki–Miyaura cross-coupling condition⁴⁶ involving catalytic tetrakis(triphenylphosphine)palladium (0) ($\text{Pd}(\text{PPh}_3)_4$) and sodium carbonate (Na_2CO_3) in 1,2-dimethoxyethane (DME) and H_2O at 100 °C for 14 h to obtain substituted indoles **18a-b**, with a yield of 50% and 87%, respectively. Ullmann type coupling reaction of intermediates **18a-b** with 2-amino substituted benzonitrile (**19**) was carried out in the presence of catalytic copper (I) iodide (CuI), *N,N'*-dimethylethylene diamine (DMEDA), and cesium carbonate (Cs_2CO_3) in 1,4-dioxane at 110 °C for 14 h^{47,48} to obtain the corresponding benzonitriles **20a-b**, with a good yield (95% and 96%). The hydrolysis of the obtained benzonitriles **20a-b** with 4 M sodium hydroxide (NaOH) and 30% hydrogen peroxide (H_2O_2) in a mixture of dimethyl sulfoxide (DMSO)^{49–51} and ethanol (EtOH) resulted in the desired benzamide compounds **11a-b**, with a yield of 65% and 97%, respectively.

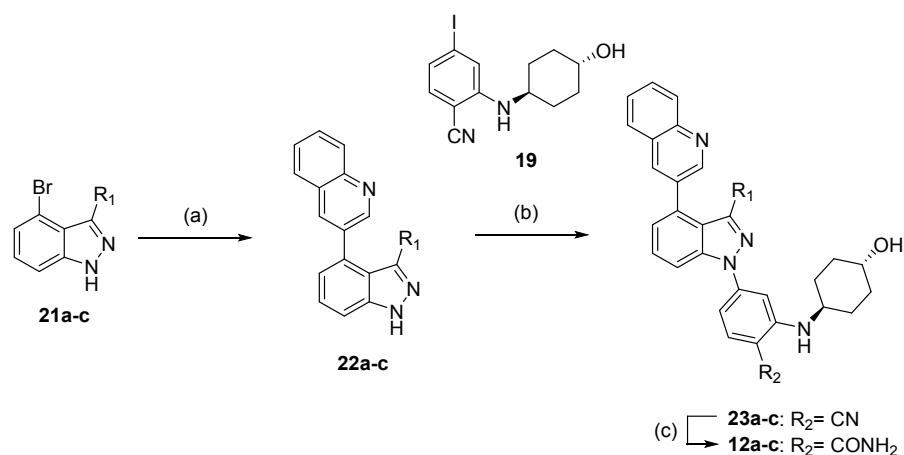
Scheme 1. Synthesis of indole derivatives 11a-b^a



^aReagents and conditions: (a) 3-quinolineboronic acid, Pd(PPh₃)₄, Na₂CO₃, DME, H₂O, 100 °C, 14 h, **18a**: 50%, **18b**: 87%; (b) **19**, CuI, DMEDA, Cs₂CO₃, 1,4-dioxane, 110 °C, 14 h, **20a**: 95%, **20b**: 96%; (c) 4 M NaOH aq., 30% H₂O₂ aq., DMSO, EtOH, 0 °C-rt, 2.5 h, **11a**: 65%, **11b**: 97%.

To examine the substitution effects of the nitrogen atom at the C-6 position (**12a**) in **11a** and the introduction of methyl (**12b**), and isopropyl (**12c**) moieties as representative alkyl substituents at the C-3 position, the compounds were synthesized as shown in Scheme 2. The synthesis of derivatives **12a-c** commenced with 3-quinolineboronic acid under Suzuki–Miyaura cross-coupling condition⁴⁶ involving catalytic [1,1'-bis(diphenylphosphino)ferrocene]dichloropalladium (II) (Pd(dppf)Cl₂·CH₂Cl₂), and Na₂CO₃ in 1,4-dioxane and H₂O at 100 °C for 3 h to obtain 3-quinoline-substituted indazoles **22a-c** (56%–94%). Ullmann-type coupling reaction of the intermediates **22a-c** with 2-amino substituted benzonitrile (**19**) was carried out in the presence of catalytic CuI, DMEDA, and tripotassium phosphate (K₃PO₄) as a base in 1,4-dioxane at 110 °C for 24 h⁴⁸ to obtain the corresponding benzonitriles **23a-c** (64%–98%). The hydrolysis of the obtained benzonitriles **23a-c** with 4 M NaOH and 30% H₂O₂ in a mixture of DMSO^{49–51} and EtOH resulted in the desired benzamide compounds **12a-c** (66%–84%).

Scheme 2. Synthesis of indazole derivatives **12a-c**^a



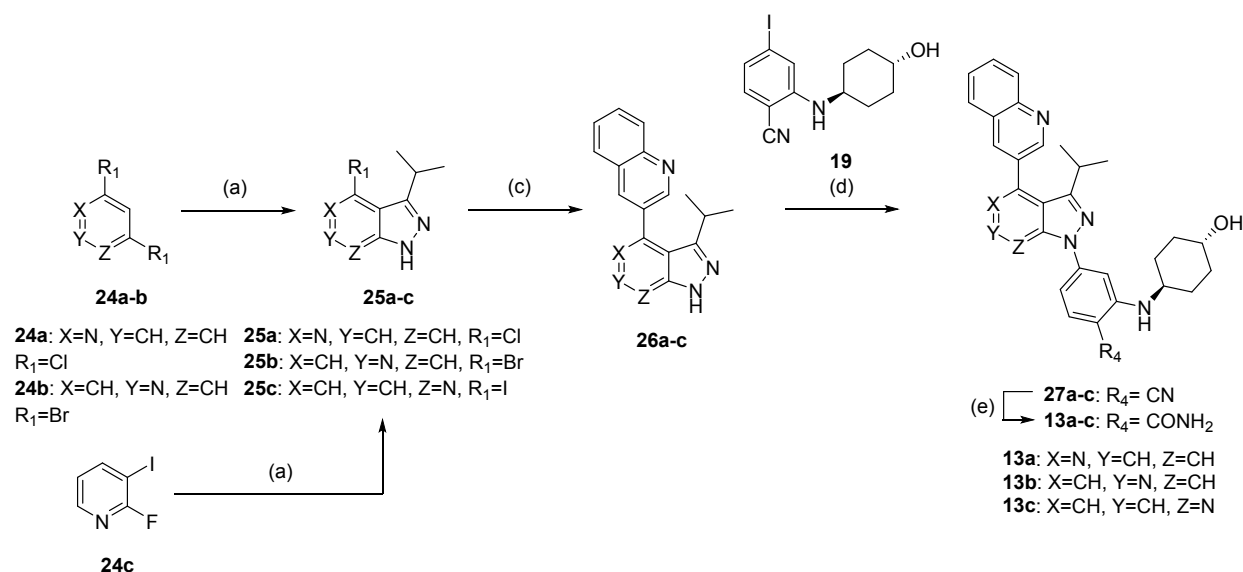
Series of **a** to **c** in compounds mean: **a**: $R_1 = \text{H}$, **b**: $R_1 = \text{Me}$, **c**: $R_1 = i\text{-Pr}$

^aReagents and conditions: (a) 3-quinolineboronic acid, $\text{Pd}(\text{dppf})\text{Cl}_2 \cdot \text{CH}_2\text{Cl}_2$, Na_2CO_3 , 1,4-dioxane, H_2O , 100 °C, 3 h, 56%–94%; (b) **19**, CuI , DMEDA, K_3PO_4 , 1,4-dioxane, 110 °C, 24 h, 64%–98%; (c) 4 M NaOH aq., 30% H_2O_2 aq., DMSO, EtOH, 0 °C–rt, 2.5 h, 66%–84%.

The 1*H*-pyrazolopyridine derivatives **13a-c** with substitution of the nitrogen atom in **12c** were synthesized as shown in Scheme 3. Lithiation of commercially available 2,4-dichloropyridine (**24a**), 3,5-dibromopyridine (**24b**), and 2-fluoro-3-iodopyridine (**24c**) was carried out in the presence of lithium diisopropylamide (LDA) in tetrahydrofuran (THF) at -78 °C, followed by alkylation with isobutyl anhydride to obtain 1-(2,4-dihalopyridin-3-yl)-2-methylpropan-1-one intermediates. Finally, intramolecular cyclization with hydrazine monohydrate was carried out to obtain C3-isopropyl substituted 1*H*-pyrazolopyridines (**25a-c**) (17%–42%). Compound **25c** was obtained by the halogen dance reaction⁵² of **24c**. The obtained 4-halo-3-isopropyl-1*H*-pyrazolopyridines (**25a-c**) were reacted with 3-quinolineboronic acid under Suzuki–Miyaura cross-coupling condition⁴⁶ involving catalytic $\text{Pd}(\text{dppf})\text{Cl}_2 \cdot \text{CH}_2\text{Cl}_2$, and Na_2CO_3 in 1,4-dioxane and H_2O at 100 °C to obtain 3-quinoline substituted pyrazolopyridines (**26a-c**) (76%–92%). In the next step, Ullmann type coupling reaction of 3-quinoline substituted pyrazolopyridines **26a-c** with 2-amino substituted benzonitrile (**19**) was carried out in the presence of catalytic CuI , DMEDA, and K_3PO_4 in 1,4-dioxane at 110 °C for 24 h⁴⁸ to obtain the corresponding

benzonitriles **27a-c** (81%–95%). The hydrolysis of the obtained benzonitriles **27a-c** with 4 M NaOH and 30% H₂O₂ in a mixture of DMSO^{49–51} and EtOH resulted in the desired benzamide compounds **13a-c** (28%–91%).

Scheme 3. Synthesis of pyrazolopyridine derivatives **13a-c**^a



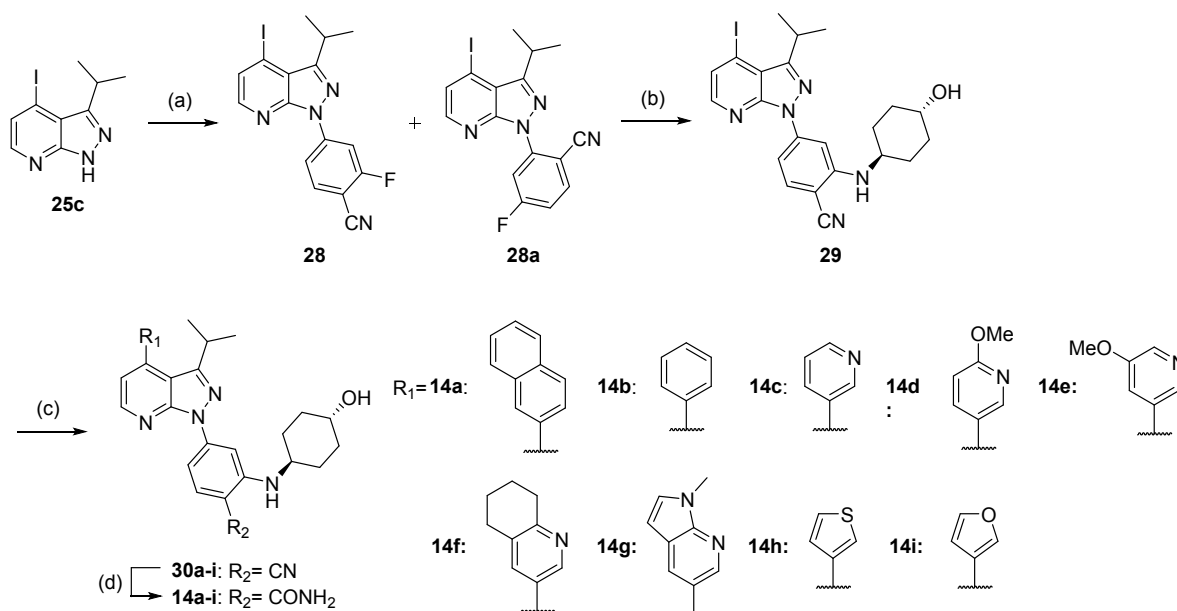
^aReagents and conditions: (a) 1) **24a-c**, DIPA, *n*-BuLi, THF, -78 °C, 15 min; 2) isobutylanhydride, -78 °C, 1 h; 3) N₂H₄ aq., 60–110 °C, 1–24 h, 17%–42%; (d) 3-quinolineboronic acid, Pd(dppf)Cl₂.CH₂Cl₂, Na₂CO₃, 1,4-dioxane, H₂O, 100 °C, 3 h, 76%–97%; (d) **19**, CuI, DMEDA, K₃PO₄, 1,4-dioxane, 110 °C, 24 h, 81%–95%; (e) 4 M NaOH aq., 30% H₂O₂ aq., DMSO, EtOH, 0 °C–rt, 2.5 h, 28%–91%.

We then focused on the 3-quinoline group of compound **13c** at the C-4 position. We selected a 3-isopropyl-1*H*-pyrazolo[3,4-*b*]pyridine in the terminal core structure, and carried out further optimization of the 3-quinoline group at the C-4 position.

The synthesis of the C-4 aryl derivatives **14a-i** is shown in scheme 4. The obtained intermediate **25c** was treated with sodium hydride (NaH) in *N,N*-dimethylformamide (DMF), and then coupled with 2,4-difluorobenzonitrile at 60 °C to obtain 2-fluorobenzonitrile **28** as a mixture of the desired product and C-2 substituted regioisomer **28a**. The obtained mixture of **28** and **28a** was reacted with *trans*-4-aminocyclohexanol in the presence of *N,N*-diisopropylethylamine

(DIPEA) in DMSO to obtain the desired intermediate **29** by column chromatography on silica gel with 15% yield in two steps. In the next step, Suzuki–Miyaura cross-coupling reaction⁴⁶ of **29** with various boronic acids or boronic acid pinacol esters mediated by catalytic $\text{Pd}(\text{PPh}_3)_4$ and Na_2CO_3 in DME and H_2O was carried out at 100 °C for 4 h to obtain 4-substituted benzonitriles **30a-i** (82%-quant.). Finally, the hydrolysis of the obtained benzonitriles **30a-i** with 4 M NaOH and 30% H_2O_2 in a mixture of DMSO^{49–51} and EtOH resulted in the desired benzamide compounds **14a-i** (75%–97%).

Scheme 4. Synthesis of pyrazolo[3,4-*b*]pyridine derivatives **14a-i**^a

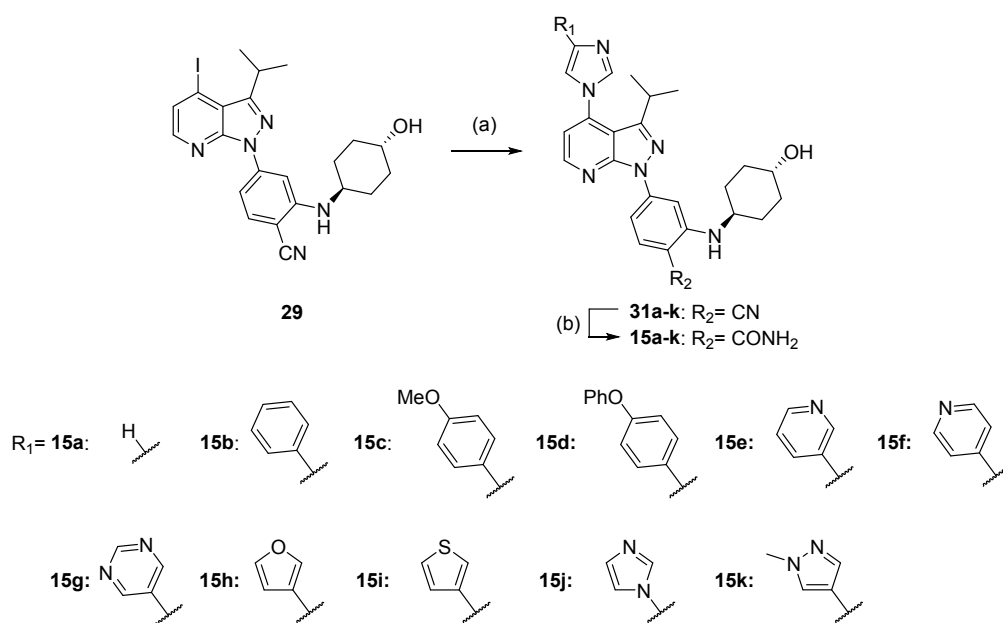


^aReagents and conditions: (a) 2,4-difluorobenzonitrile, NaH, DMF, 60 °C, 1 h; (b) *trans*-4-aminocyclohexanol, DIPEA, DMSO, 125–150 °C, 8 h, 15%, 2 steps; (c) Boronic acids or boronic acid pinacol esters, $\text{Pd}(\text{PPh}_3)_4$, Na_2CO_3 , DME, H_2O , 100 °C, 4 h, 82%-quant; (d) 4 M NaOH aq., 30% H_2O_2 aq., DMSO, EtOH, rt, 30 min, 75%–97%;

The synthesis of the 4-aryl-1*H*-imidazole derivatives **15a-k** is shown Scheme 5. Ullmann type coupling reaction of the obtained intermediate **29** with various 4-aryl-1*H*-imidazoles mediated by copper (II) oxide (CuO) nanopowder under basic conditions using potassium carbonate (K_2CO_3) in DMF was carried out at 120 °C for 20 h⁵³ to obtain 4-substituted benzonitriles **31a-k** (45%–

90%). Finally, the hydrolysis of the obtained benzonitriles **31a-k** with 4 M NaOH and 30% H₂O₂ in a mixture of DMSO^{49–51} and EtOH resulted in the desired benzamide compounds **15a-k** (50%-quant.).

Scheme 5. Synthesis of imidazole derivatives **15a-k**^a

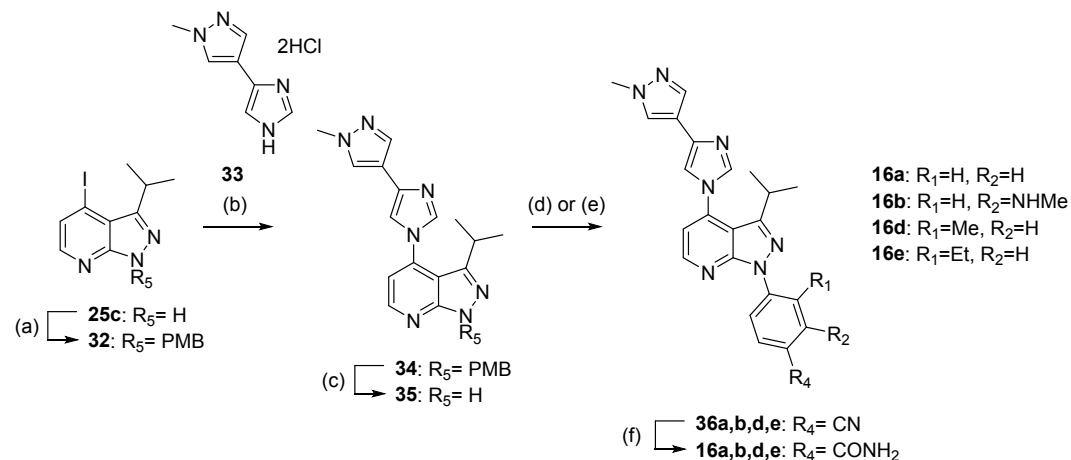


^aReagents and conditions: (a) imidazoles, CuO nanopowder, K₂CO₃, DMF, 120 °C, 20 h, 45%–90%; (b) 4 M NaOH aq., 30% H₂O₂ aq., DMSO, EtOH, 0 °C–rt, 2.5 h, 50%-quant.

To examine the substituent effects on the benzamide group, 2- or 3-substituted benzamide derivatives (**16a-e**), other than the 4-aminocyclohexanol group, were synthesized by the method shown in Scheme 6. *N*-Protection of the obtained intermediate **25c** with *p*-methoxybenzylchloride (PMBCl) in the presence of NaH in DMF at room temperature for 1 h yielded PMB protected pyrazolopyridine **32** with 91% yield. Ullmann type coupling reaction of the obtained compound **32** and 4-(1H-imidazol-4-yl)-1-methyl-1H-pyrazole dihydrochloride (**33**) was carried out in the presence of catalytic copper (I) oxide (Cu₂O), 4,7-dimethoxy-1,10-phenanthroline, polyethylene glycol (PEG), and Cs₂CO₃ in DMSO at 110 °C for 24 h⁵⁴ to obtain the desired 4-(1H-imidazol-4-yl)-1-methyl-1H-pyrazole intermediate (**34**), with a yield of 62%.

The PMB group of **34** was treated with TFA and anisole⁵⁵ to obtain pyrazolopyridine intermediate **35**, with a yield of 88%. The condensation of intermediate **37** with commercially available 4-fluorobenzonitriles was carried out in the presence of Cs₂CO₃ in DMF at 50–120 °C for 0.5–14 h to obtain 3-substituted benzonitriles **36a**, **36d**, and **36e** (81%–91%). Ullmann-type coupling reaction of the intermediate **37** with 4-iodo-2-(methylamino)benzonitrile was carried out in the presence of catalytic CuI, DMEDA, and K₃PO₄ as a base in 1,4-dioxane at 110 °C for 24 h⁴⁸ to obtain the corresponding benzonitrile **36b** (36%). Finally, the hydrolysis of the obtained benzonitriles **36a**, **36b**, **36d**, and **36e** with 4 M NaOH and 30% H₂O₂ in a mixture of DMSO^{49–51} and EtOH resulted in the desired benzamide compounds **16a**, **16b**, **16d**, and **16e** (45%–95%), respectively.

Scheme 6. Introduction of various benzamide groups to the 1*H*-imidazole-1-yl-3-isopropyl-1*H*-pyrazolo[3,4-*b*]pyridine scaffold **16a, **16b**, **16d**, **16e**^a**

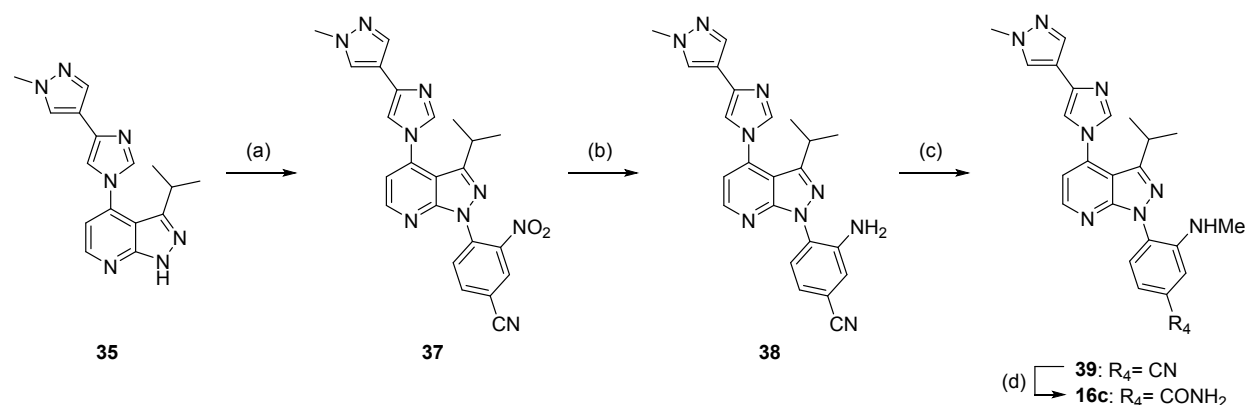


^aReagents and conditions: (a) PMBCl, NaH, DMF, 0 °C–rt, 2 h, 91%; (b) **33**, Cu₂O, 4,7-dimethoxy-1,10-phenanthroline, Cs₂CO₃, PEG, DMSO, 110 °C, 24 h, 62%; (c) TFA, anisole, reflux, 5 h, 88%; (d) benzonitriles, Cs₂CO₃, DMF, 50–120 °C, 0.5–14 h, 81%–91%; (e) 4-iodo-2-(methylamino)benzonitrile, CuI, DMEDA, K₃PO₄, 1,4-dioxane, 110 °C, 24 h, 36%; (f) 4 M NaOH aq., 30% H₂O₂ aq., DMSO, EtOH, 0 °C–rt, 2.5 h, 45%–95%.

The preparation of 3-amino substituted derivative **16c** has been summarized in Scheme 7. The condensation of intermediate **35** with commercially available 4-chloro-3-nitrobenzonitrile was

carried out in the presence of Cs_2CO_3 in DMF at 80°C for 14 h to obtain 3-nitrobenzonitrile **37** (70%). The reduction of the nitro group with iron powder and ammonium chloride (NH_4Cl) in THF, EtOH, and H_2O at 80°C for 4 h,⁵⁶ yielded 39% of 3-amino benzonitrile **38**. The monomethylation of 3-amino benzonitrile **38** was carried out in the presence of copper (II) acetate ($\text{Cu}(\text{OAc})_2$), methylboronic acid, and pyridine in 1,4-dioxane at 120°C for 2 h⁵⁷ to obtain 3-methylamino benzonitrile **39** (38%). Finally, the hydrolysis of the obtained benzonitrile **39** with 4 M NaOH and 30% H_2O_2 in a mixture of DMSO^{49–51} and EtOH resulted in the desired benzamide compound **16c** with 83% yield.

Scheme 7. Introduction of 3-(methylamino)benzamide group to the 1*H*-imidazole-1-yl-3-isopropyl-1*H*-pyrazolo[3,4-*b*]pyridine scaffold **16c^a**



^aReagents and conditions: (a) 4-chloro-3-nitrobenzonitrile, Cs_2CO_3 , DMF, 80°C , 14 h, 70%; (b) Fe, NH_4Cl , THF, EtOH, H_2O , 80°C , 4 h, 39%; (c) methylboronic acid, $\text{Cu}(\text{OAc})_2$ (II), pyridine, 1,4-dioxane, 120°C , 2 h, 38%; (d) 4 M NaOH aq., 30% H_2O_2 aq., DMSO, EtOH, 0°C , 2 h, 83%.

Conclusions

Compound **16e** (TAS-116), a potent and highly selective HSP90 α/β inhibitor with a unique binding mode was discovered by SAR-based optimization of an initial hit compound **11a**. The main findings of this study are as follows. (i) The introduction of an isopropyl group at the C-3 position of the initial hit **11a** significantly increased the HSP90 binding inhibitory activity. (ii)

The introduction of nitrogen atom at the C-2 position of the initial hit **11a** also significantly increased the HSP90 binding inhibitory activity. (iii) The introduction of nitrogen atom into the indazole ring of **12c** resulted in lower lipophilicity and hERG inhibitory activity than those by **12c**. (iv) The discovery of 4-(1*H*-imidazol-4-yl)-1-methyl-1*H*-pyrazole group, as an alternative structure of 3-quinoline group, maximized the HSP90 inhibitory activity and tumor cell growth inhibitory activity in SK-BR-3 cells. (v) Compound **16e** with favorable oral exposure in mice was discovered by optimizing the balance among the MW, TPSA, and LogD value and by improving the solubility of **15k** at pH 7.4. (vi) The X-ray co-crystal structure analysis of TAS-116 analog **16d** demonstrated a unique binding mode.

Compound **16e** also exhibited good oral absorption in mice. The oral administration of **16e** on a daily basis was well tolerated, resulting in potent antitumor effects by decreasing the amount of mutant EGFR in the NCI-H1975 (human lung cancer) xenograft model. Phase II clinical trial to evaluate the safety and efficacy of **16e** (TAS-116) is in progress.⁵⁸

Experimental Section

Measurement of HSP90-binding activity. The HSP90-binding activity was measured by the AlphaScreen competitive assay. The His-tagged HSP90 α NTD was added to a 384-well plate containing the test compounds. After reaction at room temperature for 2 h, biotin-labeled geldanamycin was added, and the mixture was incubated for a further 1 h. The bead mixture containing both nickel-chelated acceptor beads and streptavidin-coated donor beads was added. After incubation for 1 h in dark, the assay plate was measured in a PerkinElmer Envision plate reader (PerkinElmer Corporation, Waltham, MA, USA). The IC₅₀ value (nM), the concentration

of inhibitor with 50% displacement rate, was obtained from the concentration displacement rate curve.

Measurement of cell growth inhibition. Cell growth was measured using the CellTiter-Glo[®] 2.0 Assay kit (Promega Corporation, Madison, WI, USA). SK-BR-3 cells (HTB-30) purchased from the American Type Culture Collection (Manassas, VA, USA) were seeded in a 96-well plate at a concentration of 2500 cells/well. The cells were cultured in a 5% CO₂ incubator at 37 °C overnight, and the compounds were then added to the plate and incubated for further 72 h. Luminescence (CPS, count per second) was measured with a microplate reader. The ratio of treatment to control (T/C (%)), was determined using the following equation. The IC₅₀ value (nM), the concentration that exerted 50% growth inhibitory rate compared with that of the control group, was calculated from T/C (%). In this assay system, the IC₅₀ value of 17-AAG, a standard of HSP90 inhibitor, was 10 ± 1 nM.

$$\text{T/C (\%)} = [(\text{mean of CPS}_{\text{treatment}}) / (\text{mean of CPS}_{\text{control}})] \times 100$$

control: without compound (DMSO treatment)

hERG binding assay. The hERG inhibitory activity (% inhibition at 10 μM compound concentration) was measured using the Predictor[™] hERG Fluorescence Polarization Assay kit (PV5365, Invitrogen), according to the protocol of the manufacturer.

Measurement of LogD values at pH 7.4. LogD_{7.4}, which is the partition coefficient of the compounds between 1-octanol and aqueous buffer at pH 7.4, was measured by chromatography, following a previously published method.³⁶ The WATERS 2690 HPLC system with a quaternary pump (WATERS, Milford, MA, USA), PAL liquid handler (CTC Analytics, Zwingen,

Switzerland), and a SQ quadrupole mass detector (WATERS) equipped with electrospray ionization were used.

Measurement of Solubility at pH 7.4. Solubility at pH 7.4, was measured by chromatography, following a previously published method.³⁷ The WATERS Acquity UPLC system with a binary pump, plate autosampler, thermostated column compartment, sample organizer, and SQ quadrupole mass detector (WATERS, Milford, MA, USA) equipped with electrospray ionization were used.

Cloning, expression, and purification of recombinant human Hsp90 α . The cDNA of NTD of human Hsp90 α (a.a. 1–236) was subcloned into the expression vector pET19b. The construct was then transformed in *E. coli* BL21(DE3) cells (Novagen, Madison, WI, USA) in Luria broth at 37°C. Protein expression was induced with 0.01 mM isopropyl- β -d-thiogalactopyranoside (IPTG) at an optical density of 0.6 at 595 nm. The cell pellet was re-suspended in ice-cold lysis buffer containing 50 mM Tris-HCl (pH 7.5), 150 mM NaCl, and 1 mM dithiothreitol (DTT). After sonication, the disrupted debris was removed by centrifugation. The supernatant was applied on to Ni-NTA affinity gels, and the 6 \times His-Tag was removed by digestion with enterokinase in 50 mM Tris-HCl (pH 7.5), 150 mM NaCl, and 1 mM DTT for 12 h. The protein solution used for crystallization was gel filtrated in a buffer containing 50 mM Tris-HCl (pH 7.5), 50 mM NaCl, and 1 mM DTT, on a preparative grade Superdex75 column (GE Healthcare Life Sciences, Freiburg, Germany).

Co-crystal structural analysis.

The crystals of NTD of human Hsp90 α in complex with compound **16d** were grown by the hanging-drop vapor diffusion method in a solution of PEG6000, 200 mmol/L NaCl, and 50

mmol/L Tris (pH 7.5) at 4°C. The protein was concentrated to 25 mg/mL and 2 mmol/L compound was added. For data collection, the crystals were transferred to drops containing equivalent amount of mother liquor with 25% glycerol. The diffraction data were collected in-house using a Rigaku MicroMax-007 generator with an RAXIS IV++ imaging plate detector. The data were processed using the program iMOSFLM⁵⁹ from the CCP4 suite.⁶⁰ The space group was $P2_1$. The structure of NTD of human Hsp90 α complexed with inhibitor was determined by molecular replacement using the program MOLREP.⁶¹ The search model was based on NTD of Hsp90 structure (PDB ID: 3WQ9). The structure of NTD of human Hsp90 α in complex with compound **16d** was refined using REFMAC5.⁶² Manual re-building of the models and electron density map interpretation were carried out using COOT.⁶³ The final model had the following R values: $R_{\text{work}} = 20.7\%$ and $R_{\text{free}} = 25.7\%$. A summary of statistics from the data collection and refinement is given in Table S1.

Animal experiments. All animal experiments were performed with the approval of the Institutional Animal Care and Use Committee of the Taiho Pharmaceutical Co. Ltd. and carried out according to the Guidelines for Animal Experiments of the Taiho Pharmaceutical Co. Ltd.

Pharmacokinetic analysis. The experiments were conducted with 8–11-week-old male Balb/c-A mice. Five test compounds were orally administered to the mice at a dose of 50 mg/kg in a vehicle containing 0.5% (w/v) hydroxypropyl methylcellulose (Metolose 60SH-50; Shin-Etsu Chemical Co. Ltd., Tokyo, Japan). Blood samples were collected over a 6-h period after treatment. After centrifugation, the plasma concentration of five test compounds was determined by liquid chromatography-tandem mass spectrometry. The pharmacokinetic parameters were calculated by the non-compartmental methods using Phoenix® WinNonlin® (Certara LP, Princeton, NJ, USA).

***In vivo* studies.** NCI-H1975 cells (purchased from ATCC, CRL-5908) were subcutaneously implanted into six-week-old male BALB/cAJcl-nu/nu mice (CLEA Japan, Inc., Kanagawa, Japan) and allowed to grow. Six animals were assigned to each treatment group, and TAS-116 formulated in 0.5% (w/v) hydroxypropyl methylcellulose in H₂O was administered orally every day. The tumor volume was measured using the following formula: $[\text{length} \times (\text{width})^2] / 2$. Statistical significance was calculated by Dunnett's test to assess the difference in tumor volume between the control and treated groups. Differences with a *P* value < 0.05 were considered statistically significant. For the pharmacodynamic analysis, the tumors were harvested at the indicated time points after the administration of TAS-116. To evaluate the amount and phosphorylation status of proteins, the excised tumors were homogenized in lysing matrix D (MP Biomedicals, LLC, Santa Ana, CA, USA) containing lysis buffer.

Western blot analysis. The proteins were separated by SDS-PAGE and transferred on to polyvinylidene fluoride membranes (Bio-Rad Laboratories Inc., Hercules, CA, USA). The membranes were blocked with Blocking One or Blocking One P blocking reagent (Nacalai Tesque Inc., Kyoto, Japan) and probed with appropriate primary antibodies. The membranes were then incubated with horseradish peroxidase-linked secondary antibodies (Cell Signaling Technology Inc., Danvers, MA, USA), and the proteins were visualized by means of luminol-based enhanced chemiluminescence (Thermo Fisher Scientific Inc., Waltham, MA, USA). The luminescent images were captured using an LAS-3000 imaging system (Fuji Photo Film Co. Ltd., Tokyo, Japan). The primary antibodies used to detect specific proteins were purchased as follows: EGFR (#2242), phospho-p44/42 MAPK (#4370), p44/ 42 MAPK (#9102), phospho-AKT (#4060), AKT (#4691), phospho-S6 Ribosomal Protein (Ser235/236; #4858), S6

Ribosomal Protein (#2217), anti-GAPDH (#2118) from Cell Signaling Technology Inc. (Danvers, MA, USA).

General chemistry information. All solvents and reagents were obtained from commercial sources and were used as received. All reactions were monitored by ultra-performance liquid chromatography-mass spectrometry (UPLC-MS). The UPLC-MS analysis was performed using ACQUITY™ UPLC system (WATERS Corporation, Milford, MA, USA) and Micromass ZQ Mass Spectrometer (WATERS Corporation, Milford, MA, USA) equipped with electrospray ionization in the ESI positive mode. The column used was an Acquity UPLC® BEH C18-column (2.1 mm × 50 mm, 1.7 μm, Waters Corporation) at 40 °C with a flow rate of 0.5 mL/min. Mobile phase A was 0.5% formic acid in water. Mobile phase B was 0.5% formic acid in acetonitrile, which was increased linearly from 5% to 95% over 2 min, 95% to 98% over the next 1.4 min, after which the column was equilibrated to 5% for 1.5 min and detected at 254 nm. Column chromatography was also performed on a Biotage Isolera™ purification system using prepacked Biotage® SNAP Ultra (SI, particle size 25 μm). The yields were not optimized. All the final test compounds were purified to > 95% chemical purity as measured by UPLC-MS. The proton nuclear magnetic resonance (¹H NMR) spectra were recorded on a Varian Mercury-400 (400 MHz), JEOL JNM-AL400 (400 MHz) instrument. All the ¹H NMR spectra were consistent with the proposed structures. All proton shifts are provided in parts per million (ppm) downfield from the appropriate internal deuterated solvent peak or tetramethylsilane (δ) as the internal standard in deuterated solvent, and the coupling constants (J) are in hertz (Hz). The NMR data are reported as follows: chemical shift, multiplicity (s, singlet; d, doublet; t, triplet; q, quartet; spt, septet; m, multiplet; dd, doublet of doublets; td, triplet of doublets; and brs, broad singlet), coupling constants, and integration. The broad peaks of the protons of hydroxyl and amino groups are not

always indicated. The high resolution mass spectral analysis (HRMS) was carried out using ACQUITY UPLC I-Class and Vion IMS QToF (WATERS Corporation, Milford, MA, USA).

2-((*trans*-4-Hydroxycyclohexyl)amino)-4-(4-(quinolin-3-yl)-1*H*-indol-1-yl)benzamide (11a).

To a solution of **20a** (222 mg, 0.48 mmol), DMSO (0.55 mL), and EtOH (2.2 mL), 4 M NaOH aq. (0.24 mL, 0.96 mmol), and 30% H₂O₂ aq. (0.11 mL, 0.96 mmol) were added on ice. After being stirred for 30 min at 0 °C, the reaction mixture was allowed to warm to room temperature and stirred for 2 h. The reaction mixture was quenched with 2.2 mL of 10% Na₂S₂O₃ aq. on ice. Water (11 mL) was added to the mixture, and the mixture was stirred at room temperature for 10 min. The resulting precipitate was collected by filtration. The precipitate was washed with water and dried under vacuum to obtain 148 mg (65%) of **11a** as a white powder. UPLC-MS (ESI) *m/z*=477.2 [M+H]⁺, *t_R*=1.51 min. UPLC purity 97.45%. ¹H NMR (400 MHz, DMSO-*d*₆) δ 1.18–1.38 (m, 4H), 1.82 (br d, *J*=10.2 Hz, 2H), 1.93–2.06 (m, 2H), 3.37–3.55 (m, 2H), 4.57 (d, *J*=4.4 Hz, 1H), 6.75 (dd, *J*=8.3, 2.0 Hz, 1H), 6.84 (d, *J*=2.0 Hz, 1H), 6.90 (d, *J*=3.4 Hz, 1H), 7.24 (brs, 1H), 7.38–7.45 (m, 2H), 7.66–7.73 (m, 2H), 7.79–7.85 (m, 3H), 7.94 (brs, 1H), 8.06–8.17 (m, 2H), 8.51 (d, *J*=7.8 Hz, 1H), 8.65 (d, *J*=2.2 Hz, 1H), 9.20–9.28 (m, 1H). HRMS calcd for C₃₀H₂₈N₄O₂ 477.2285 [M+H]⁺, found 477.2286.

The following compound **11b** was prepared from the corresponding indole **17b** by a method similar to that described for **11a**.

2-((*trans*-4-Hydroxycyclohexyl)amino)-4-(3-methyl-4-(quinolin-3-yl)-1*H*-indol-1-yl)benzamide (11b). Yield 81% (3 steps), white powder. UPLC-MS (ESI) *m/z*=491.2 [M+H]⁺, *t_R*=1.58 min. UPLC purity 98.83%. ¹H NMR (400 MHz, DMSO-*d*₆) δ 1.15–1.37 (m, 4H), 1.77–1.85 (m, 5H), 1.89–2.06 (m, 2H), 4.54 (d, *J*=4.0 Hz, 1H), 6.68 (dd, *J*=8.4, 2.20 Hz, 1H), 6.77 (d,

$J=1.8$ Hz, 1H), 7.10 (d, $J=7.3$ Hz, 1H), 7.19 (brs, 1H), 7.24–7.37 (m, 1H), 7.55 (s, 1H), 7.63–7.71 (m, 2H), 7.76–7.85 (m, 2H), 7.88 (brs, 1H), 8.04–8.12 (m, 2H), 8.30 (s, 1H), 8.41 (d, $J=2.2$ Hz, 1H), 8.47 (d, $J=7.7$ Hz, 1H), 8.99 (d, $J=2.2$ Hz, 1H). HRMS calcd for $C_{31}H_{30}N_4O_2$ 491.2447 $[M+H]^+$, found 491.2447.

2-((*trans*-4-Hydroxycyclohexyl)amino)-4-(4-(quinolin-3-yl)-1*H*-indazol-1-yl)benzamide

(12a). To a solution of **23a** (300 mg, 0.65 mmol), DMSO (0.75 mL), and EtOH (3 mL), 4 M NaOH aq. (0.41 mL, 1.63 mmol), and 30% H_2O_2 aq. (0.19 mL, 1.63 mmol) were added on ice. After being stirred for 30 min at 0 °C, the reaction mixture was allowed to warm to room temperature and stirred for 2 h. The reaction mixture was quenched with 10% $Na_2S_2O_3$ aq. (3 mL) on ice and diluted with $CHCl_3$. The mixture was extracted with $CHCl_3$. The organic layer was washed with 5% NaCl aq., dried over $MgSO_4$, and concentrated *in vacuo*. The residue was purified by column chromatography (eluents, 12%–100% EtOAc in hexane and 0%–20% MeOH in EtOAc) to obtain 208 mg (67%) of **12a** as a white powder. UPLC-MS (ESI) $m/z=478.3$ $[M+H]^+$, $t_R=1.47$ min. UPLC purity 99.84%. 1H NMR (400 MHz, $DMSO-d_6$) δ 1.20–1.40 (m, 4H), 1.78–1.92 (m, 2H), 1.97–2.11 (m, 2H), 3.34–3.44 (m, 1H), 3.44–3.55 (m, 1H), 4.55 (d, $J=4.2$ Hz, 1H), 6.94 (dd, $J=8.5$, 2.0 Hz, 1H), 7.03 (d, $J=1.7$ Hz, 1H), 7.23 (brs, 1H), 7.61 (d, $J=7.1$ Hz, 1H), 7.66–7.76 (m, 2H), 7.81–7.90 (m, 2H), 7.90–8.02 (m, 2H), 8.13 (d, $J=8.5$ Hz, 1H), 8.17 (d, $J=8.1$ Hz, 1H), 8.50 (d, $J=7.8$ Hz, 1H), 8.63 (s, 1H), 8.79 (d, $J=2.2$ Hz, 1H), 9.31 (d, $J=2.2$ Hz, 1H). HRMS calcd for $C_{29}H_{27}N_5O_2$ 478.2238 $[M+H]^+$, found 478.2241.

The following compounds (**12b**, **12c**) were prepared from the corresponding indazoles (**21b**, **21c**) by a method similar to that described for **12a**.

2-((*trans*-4-Hydroxycyclohexyl)amino)-4-(3-methyl-4-(quinolin-3-yl)-1*H*-indazol-1-yl)benzamide (12b). Yield 46% (3 steps), white powder. UPLC-MS (ESI) $m/z=492.1$ $[M+H]^+$, $t_R=1.50$ min. UPLC purity 99.31%. 1H NMR (400 MHz, DMSO- d_6) δ 1.18–1.37 (m, 4H), 1.78–1.87 (m, 2H), 1.99–2.08 (m, 2H), 2.13 (s, 3H), 3.32–3.40 (m, 1H), 3.43–3.53 (m, 1H), 4.55 (d, $J=4.0$ Hz, 1H), 6.87 (dd, $J=8.4$, 1.8 Hz, 1H), 6.96 (d, $J=2.2$ Hz, 1H), 7.19 (brs, 1H), 7.27 (d, $J=7.0$ Hz, 1H), 7.57–7.63 (m, 1H), 7.66–7.72 (m, 1H), 7.78–7.86 (m, 2H), 7.89 (d, $J=8.4$ Hz, 2H), 8.11 (t, $J=6.9$ Hz, 2H), 8.49 (d, $J=7.1$ Hz, 1H), 8.52 (s, 1H), 9.05 (d, $J=2.2$ Hz, 1H). HRMS calcd for $C_{30}H_{29}N_5O_2$ 492.2394 $[M+H]^+$, found 492.2398.

2-((*trans*-4-Hydroxycyclohexyl)amino)-4-(3-isopropyl-4-(quinolin-3-yl)-1*H*-indazol-1-yl)benzamide (12c). Yield 31% (3 steps), white powder. UPLC-MS (ESI) $m/z=520.2$ $[M+H]^+$, $t_R=1.73$ min. UPLC purity 99.39%. 1H NMR (400 MHz, DMSO- d_6) δ 1.03 (d, $J=6.8$ Hz, 6H), 1.21–1.38 (m, 4H), 1.79–1.90 (m, 2H), 1.99–2.09 (m, 2H), 2.83 (spt, $J=6.7$ Hz, 1H), 3.32–3.41 (m, 1H), 3.46–3.55 (m, 1H), 4.55 (d, $J=4.4$ Hz, 1H), 6.89 (dd, $J=8.4$, 2.1 Hz, 1H), 7.01 (d, $J=2.2$ Hz, 1H), 7.16–7.30 (m, 2H), 7.59–7.65 (m, 1H), 7.69–7.75 (m, 1H), 7.80–7.97 (m, 4H), 8.11 (d, $J=7.6$ Hz, 1H), 8.14 (d, $J=8.5$ Hz, 1H), 8.49 (d, $J=7.6$ Hz, 1H), 8.55 (d, $J=2.0$ Hz, 1H), 9.06 (d, $J=2.2$ Hz, 1H). HRMS calcd for $C_{32}H_{33}N_5O_2$ 520.2707 $[M+H]^+$, found 520.2710.

2-((*trans*-4-Hydroxycyclohexyl)amino)-4-(3-isopropyl-4-(quinolin-3-yl)-1*H*-pyrazolo[4,3-*c*]pyridin-1-yl)benzamide (13a). To a solution of **27a** (30 mg, 0.06 mmol), DMSO (0.15 mL), and EtOH (0.3 mL), 4 M NaOH aq. (44.8 μ L, 0.18 mmol), and 30% H_2O_2 aq. (20.3 μ L, 0.18 mmol) were added on ice. After being stirred for 30 min at 0 $^\circ$ C, the reaction mixture was allowed to warm to room temperature and stirred for 2 h. The reaction mixture was quenched with 10% $Na_2S_2O_3$ aq. (0.3 mL) on ice and diluted with $CHCl_3$. The mixture was extracted with $CHCl_3$. The organic layer was washed with 5% NaCl aq., dried over $MgSO_4$, and concentrated *in*

vacuo. The residue was purified by column chromatography (eluent, 12%–100% EtOAc in hexane and 0%–20% MeOH in EtOAc) to obtain 28 mg (91%) of **13a** as a white powder. UPLC-MS (ESI) $m/z=521.3$ $[M+H]^+$, $t_R=1.39$ min. UPLC purity 99.41%. 1H NMR (400 MHz, DMSO- d_6) δ 1.06 (d, $J=6.6$ Hz, 6H), 1.19–1.38 (m, 4H), 1.76–1.89 (m, 2H), 1.95–2.10 (m, 2H), 3.05 (spt, $J=6.8$ Hz, 1H), 3.33–3.42 (m, 1H), 3.44–3.52 (m, 1H), 4.55 (d, $J=4.0$ Hz, 1H), 6.89 (dd, $J=8.4$, 1.8 Hz, 1H), 7.01 (d, $J=1.8$ Hz, 1H), 7.24 (brs, 1H), 7.69–7.74 (m, 1H), 7.80–7.97 (m, 3H), 8.14 (dd, $J=8.1$, 2.9 Hz, 2H), 8.48 (d, $J=7.7$ Hz, 1H), 8.60 (d, $J=5.9$ Hz, 1H), 8.70 (d, $J=2.2$ Hz, 1H), 9.18 (d, $J=2.2$ Hz, 1H). HRMS calcd for $C_{31}H_{32}N_6O_2$ 521.2665 $[M+H]^+$, found 521.2663.

The following compounds (**13b**, **13c**) were prepared from the corresponding pyridines (**26b**, **26c**) by a method similar to that described for **13a**.

2-((trans-4-Hydroxycyclohexyl)amino)-4-(3-isopropyl-4-(quinolin-3-yl)-1H-pyrazolo[3,4-c]pyridin-1-yl)benzamide (13b). Yield 10% (4 steps), white powder. UPLC-MS (ESI) $m/z=521.1$ $[M+H]^+$, $t_R=1.54$ min. UPLC purity 96.62%. 1H NMR (400 MHz, DMSO- d_6) δ 1.05 (d, $J=6.6$ Hz, 6H), 1.18–1.38 (m, 4H), 1.76–1.90 (m, 2H), 1.94–2.12 (m, 2H), 2.94 (spt, $J=6.8$ Hz, 1H), 3.35–3.52 (m, 2H), 4.55 (d, $J=4.4$ Hz, 1H), 6.96 (dd, $J=8.4$, 2.2 Hz, 1H), 7.08 (d, $J=1.8$ Hz, 1H), 7.23 (brs, 1H), 7.69–7.75 (m, 1H), 7.81–7.91 (m, 2H), 7.94 (brs, 1H), 8.11 (br d, $J=7.7$ Hz, 1H), 8.14 (br d, $J=8.4$ Hz, 1H), 8.36 (s, 1H), 8.49 (d, $J=7.7$ Hz, 1H), 8.64 (d, $J=2.2$ Hz, 1H), 9.11 (d, $J=2.2$ Hz, 1H), 9.35 (brs, 1H). HRMS calcd for $C_{31}H_{32}N_6O_2$ 521.2665 $[M+H]^+$, found 521.2662.

2-((trans-4-Hydroxycyclohexyl)amino)-4-(3-isopropyl-4-(quinolin-3-yl)-1H-pyrazolo[3,4-b]pyridin-1-yl)benzamide (13c). Yield 36% (4 steps), white powder. UPLC-MS (ESI) $m/z=521.2$ $[M+H]^+$, $t_R=1.76$ min. UPLC purity 98.58%. 1H NMR (400 MHz, DMSO- d_6) δ 1.03

(d, $J=7.0$ Hz, 6H), 1.20–1.40 (m, 4H), 1.83–1.92 (m, 2H), 2.03–2.18 (m, 2H), 2.95 (spt, $J=6.9$ Hz, 1H), 3.25–3.36 (m, 1H), 3.45–3.54 (m, 1H), 4.58 (d, $J=4.4$ Hz, 1H), 7.14 (brs, 1H), 7.41 (d, $J=4.8$ Hz, 1H), 7.44–7.48 (m, 1H), 7.70–7.79 (m, 2H), 7.80–7.91 (m, 3H), 8.14 (t, $J=9.5$ Hz, 2H), 8.41 (d, $J=7.3$ Hz, 1H), 8.68 (d, $J=2.2$ Hz, 1H), 8.74 (d, $J=4.8$ Hz, 1H), 9.13 (d, $J=2.2$ Hz, 1H). HRMS calcd for $C_{31}H_{32}N_6O_2$ 521.2665 $[M+H]^+$, found 521.2665.

2-((*trans*-4-Hydroxycyclohexyl)amino)-4-(3-isopropyl-4-(naphthalen-2-yl)-1*H*-pyrazolo[3,4-*b*]pyridin-1-yl)benzamide (14a). To a solution of **30a** (44 mg, 0.087 mmol), DMSO (0.22 mL), and EtOH (0.44 mL), 4 M NaOH aq. (66 μ L, 0.26 mmol) and 30% H_2O_2 aq. (30 μ L, 0.26 mmol) were added under ice-cooling. After being stirred for 30 min at 0 °C, the reaction mixture was allowed to warm to room temperature and stirred for 2 h. The reaction mixture was quenched with 10% $Na_2S_2O_3$ aq. (0.44 mL) on ice and diluted with $CHCl_3$. The mixture was extracted with $CHCl_3$. The organic layer was washed with 5% NaCl aq., dried over $MgSO_4$, and concentrated *in vacuo*. The residue was purified by column chromatography (eluent, 12%–100% EtOAc in hexane and 0%–20% MeOH in EtOAc) to obtain 42 mg (92%) of **14a** as a white powder. UPLC-MS (ESI) $m/z=520.3$ $[M+H]^+$, $t_R=2.14$ min. UPLC purity 99.39%. 1H NMR (400 MHz, $DMSO-d_6$) δ 1.01 (d, $J=7.0$ Hz, 6H), 1.20–1.40 (m, 4H), 1.79–1.96 (m, 2H), 2.04–2.17 (m, 2H), 2.96–3.08 (m, 1H), 3.25–3.36 (m, 1H), 3.46–3.54 (m, 1H), 4.59 (d, $J=4.4$ Hz, 1H), 7.13 (brs, 1H), 7.31 (d, $J=4.4$ Hz, 1H), 7.47 (dd, $J=8.8, 1.8$ Hz, 1H), 7.61 (d, $J=9.5$ Hz, 2H), 7.71 (dd, $J=8.4, 1.5$ Hz, 1H), 7.77 (d, $J=8.8$ Hz, 1H), 7.83 (brs, 1H), 7.88 (d, $J=1.8$ Hz, 1H), 8.02–8.06 (m, 2H), 8.09 (d, $J=8.4$ Hz, 1H), 8.12–8.16 (m, 1H), 8.42 (d, $J=7.0$ Hz, 1H), 8.68 (d, $J=4.8$ Hz, 1H). HRMS calcd for $C_{32}H_{33}N_5O_2$ 520.2707 $[M+H]^+$, found 520.2707.

The following compounds (**14b**, **14c**, **14d**, **14e**, **14f**, **14g**, **14h**, **14i**) were prepared from **31** and the corresponding boronic acids by a method similar to that described for **14a**.

2-((trans-4-Hydroxycyclohexyl)amino)-4-(3-isopropyl-4-phenyl-1H-pyrazolo[3,4-b]pyridin-1-yl)benzamide (14b). Yield 74% (2 steps), white powder. UPLC-MS (ESI) $m/z=470.2$ $[M+H]^+$, $t_R=1.98$ min. UPLC purity 100%. 1H NMR (400 MHz, DMSO- d_6) δ 1.06 (d, $J=6.8$ Hz, 6H), 1.21–1.40 (m, 4H), 1.84–1.94 (m, 2H), 2.07–2.16 (m, 2H), 2.98–3.07 (m, 1H), 3.27–3.37 (m, 1H), 3.47–3.56 (m, 1H), 4.58 (d, $J=4.4$ Hz, 1H), 7.13 (brs, 1H), 7.22 (d, $J=4.6$ Hz, 1H), 7.47 (dd, $J=8.8, 2.0$ Hz, 1H), 7.58 (s, 5H), 7.71–7.95 (m, 3H), 8.42 (d, $J=7.1$ Hz, 1H), 8.66 (d, $J=4.9$ Hz, 1H). HRMS calcd for $C_{28}H_{31}N_5O_2$ 470.2551 $[M+H]^+$, found 470.2547.

2-((trans-4-Hydroxycyclohexyl)amino)-4-(3-isopropyl-4-(pyridin-3-yl)-1H-pyrazolo[3,4-b]pyridin-1-yl)benzamide (14c). Yield 97% (2 steps), white powder. UPLC-MS (ESI) $m/z=471.0$ $[M+H]^+$, $t_R=1.47$ min. UPLC purity 97.46%. 1H NMR (400 MHz, DMSO- d_6) δ 1.06 (d, $J=7.0$ Hz, 6H), 1.15–1.40 (m, 4H), 1.79–1.95 (m, 2H), 2.00–2.18 (m, 2H), 2.84–3.02 (m, 1H), 3.25–3.55 (m, 1H), 4.57 (d, $J=4.4$ Hz, 1H), 7.12 (brs, 1H), 7.27 (d, $J=4.8$ Hz, 1H), 7.41–7.65 (m, 5H), 7.72–7.90 (m, 3H), 8.06 (d, $J=7.7$ Hz, 1H), 8.40 (d, $J=7.3$ Hz, 1H), 8.69 (d, $J=4.8$ Hz, 1H), 8.72–8.84 (m, 2H). HRMS calcd for $C_{27}H_{30}N_6O_2$ 471.2508 $[M+H]^+$, found 471.2510.

2-((trans-4-Hydroxycyclohexyl)amino)-4-(3-isopropyl-4-(6-methoxypyridin-3-yl)-1H-pyrazolo[3,4-b]pyridin-1-yl)benzamide (14d). Yield 93% (2 steps), white powder. UPLC-MS (ESI) $m/z=501.5$ $[M+H]^+$, $t_R=1.77$ min. UPLC purity 99.29%. 1H NMR (400 MHz, DMSO- d_6) δ 1.09 (d, $J=6.6$ Hz, 6H), 1.18–1.39 (m, 4H), 1.83–1.91 (m, 2H), 2.01–2.15 (m, 2H), 2.97–3.07 (m, 1H), 3.26–3.34 (m, 1H), 3.43–3.54 (m, 1H), 3.94 (s, 3H), 4.58 (d, $J=4.4$ Hz, 1H), 7.01 (d, $J=8.4$ Hz, 1H), 7.12 (brs, 1H), 7.23 (d, $J=4.8$ Hz, 1H), 7.44 (dd, $J=8.6, 2.0$ Hz, 1H), 7.75 (d, $J=8.8$ Hz,

1H), 7.83 (d, $J=2.2$ Hz, 2H), 7.97 (dd, $J=8.6$, 2.4 Hz, 1H), 8.38–8.42 (m, 2H), 8.65 (d, $J=4.8$ Hz, 1H). HRMS calcd for $C_{28}H_{32}N_6O_3$ 501.2609 $[M+H]^+$, found 501.2610.

2-((*trans*-4-Hydroxycyclohexyl)amino)-4-(3-isopropyl-4-(5-methoxypyridin-3-yl)-1H-pyrazolo[3,4-*b*]pyridin-1-yl)benzamide (14e). Yield 78% (2 steps), white powder. UPLC-MS (ESI) $m/z=501.1$ $[M+H]^+$, $t_R=1.52$ min. UPLC purity 97.78%. 1H NMR (400 MHz, DMSO- d_6) δ 1.09 (d, $J=7.0$ Hz, 6H), 1.19–1.39 (m, 4H), 1.81–1.91 (m, 2H), 2.04–2.13 (m, 2H), 2.90–3.01 (m, 1H), 3.27–3.32 (m, 1H), 3.46–3.55 (m, 1H), 3.89 (s, 3H), 4.58 (d, $J=4.4$ Hz, 1H), 7.13 (brs, 1H), 7.29 (d, $J=4.8$ Hz, 1H), 7.44 (dd, $J=8.8$, 2.2 Hz, 1H), 7.66–7.69 (m, 1H), 7.71–7.89 (m, 3H), 8.35–8.37 (m, 1H), 8.38–8.42 (m, 1H), 8.45–8.47 (m, 1H), 8.68 (d, $J=4.8$ Hz, 1H). HRMS calcd for $C_{28}H_{32}N_6O_3$ 501.2614 $[M+H]^+$, found 501.2617.

2-((*trans*-4-Hydroxycyclohexyl)amino)-4-(3-isopropyl-4-(5,6,7,8-tetrahydroquinolin-3-yl)-1H-pyrazolo[3,4-*b*]pyridin-1-yl)benzamide (14f). Yield 83% (2 steps), white powder. UPLC-MS (ESI) $m/z=525.2$ $[M+H]^+$, $t_R=1.41$ min. UPLC purity 99.60%. 1H NMR (400 MHz, DMSO- d_6) δ 1.10 (d, $J=6.6$ Hz, 6H), 1.17–1.41 (m, 4H), 1.75–1.83 (m, 2H), 1.83–1.93 (m, 4H), 2.09 (d, $J=11.0$ Hz, 2H), 2.82 (t, $J=6.1$ Hz, 2H), 2.90 (t, $J=6.4$ Hz, 2H), 2.99 (spt, $J=6.8$ Hz, 1 H), 3.29–3.34 (m, 1H), 3.43–3.56 (m, 1H), 4.58 (d, $J=4.0$ Hz, 1H), 7.13 (brs, 1H), 7.22 (d, $J=4.8$ Hz, 1H), 7.44 (dd, $J=8.8$, 1.8 Hz, 1H), 7.67–7.89 (m, 4H), 8.40 (d, $J=7.0$ Hz, 1H), 8.48 (d, $J=2.2$ Hz, 1H), 8.65 (d, $J=4.8$ Hz, 1H). HRMS calcd for $C_{31}H_{36}N_6O_2$ 525.2973 $[M+H]^+$, found 525.2975.

2-((*trans*-4-Hydroxycyclohexyl)amino)-4-(3-isopropyl-4-(1-methyl-1H-pyrrolo[2,3-*b*]pyridin-5-yl)-1H-pyrazolo[3,4-*b*]pyridin-1-yl)benzamide (14g). Yield 75% (2 steps), white powder. UPLC-MS (ESI) $m/z=524.2$ $[M+H]^+$, $t_R=1.69$ min. UPLC purity 99.11%. 1H NMR (400 MHz, DMSO- d_6) δ 1.03 (d, $J=7.0$ Hz, 6H), 1.20–1.39 (m, 4H), 1.81–1.92 (m, 2H), 2.05–2.16 (m,

2H), 3.00 (spt, $J=6.7$ Hz, 1H), 3.26–3.81 (m, 3H), 3.90 (s, 3H), 6.58 (d, $J=3.3$ Hz, 1H), 7.12 (brs, 1H), 7.26 (d, $J=4.8$ Hz, 1H), 7.47 (dd, $J=8.6, 2.0$ Hz, 1H), 7.65 (d, $J=3.3$ Hz, 1H), 7.72–7.91 (m, 3H), 8.20 (d, $J=2.2$ Hz, 1H), 8.44 (d, $J=1.8$ Hz, 1H), 8.65 (d, $J=4.4$ Hz, 1H). HRMS calcd for $C_{30}H_{33}N_7O_2$ 524.2774 $[M+H]^+$, found 524.2776.

2-((*trans*-4-Hydroxycyclohexyl)amino)-4-(3-isopropyl-4-(thiophen-3-yl)-1*H*-pyrazolo[3,4-*b*]pyridin-1-yl)benzamide (14h). Yield 84% (2 steps), white powder. UPLC-MS (ESI) $m/z=476.4$ $[M+H]^+$, $t_R=1.91$ min. UPLC purity 99.08%. 1H NMR (400 MHz, DMSO- d_6) δ 1.10 (d, $J=6.6$ Hz, 6H), 1.20–1.38 (m, 4H), 1.80–1.97 (m, 2H), 2.02–2.17 (m, 2H), 3.16–3.24 (m, 1H), 3.25–3.34 (m, 1H), 3.45–3.55 (m, 1H), 4.58 (d, $J=4.4$ Hz, 1H), 7.11 (brs, 1H), 7.20–7.24 (m, 1H), 7.40–7.48 (m, 2H), 7.72–7.90 (m, 5H), 8.40 (d, $J=7.0$ Hz, 1H), 8.61 (d, $J=4.8$ Hz, 1H). HRMS calcd for $C_{26}H_{29}N_5O_2S$ 476.2115 $[M+H]^+$, found 476.2116.

4-(4-(furan-3-yl)-3-isopropyl-1*H*-pyrazolo[3,4-*b*]pyridin-1-yl)-2-((*trans*-4-hydroxycyclohexyl)amino)benzamide (14i). Yield 85% (2 steps), white powder. UPLC-MS (ESI) $m/z=460.3$ $[M+H]^+$, $t_R=1.79$ min. UPLC purity 98.14%. 1H NMR (400 MHz, DMSO- d_6) δ 1.15–1.40 (m, 10H), 1.81–1.93 (m, 2H), 2.04–2.15 (m, 2H), 3.17–3.43 (m, 2H), 3.45–3.54 (m, 1H), 4.58 (brs, 1 H), 6.90–6.92 (m, 1H), 7.12 (brs, 1H), 7.21 (d, $J=4.8$ Hz, 1H), 7.44 (dd, $J=8.6, 2.0$ Hz, 1H), 7.72–7.86 (m, 3H), 7.86–7.95 (m, 1H), 8.14 (brs, 1H), 8.40 (d, $J=7.0$ Hz, 1H), 8.59 (d, $J=4.8$ Hz, 1H). HRMS calcd for $C_{26}H_{29}N_5O_3$ 460.2343 $[M+H]^+$, found 460.2343.

4-(4-(1*H*-imidazol-1-yl)-3-isopropyl-1*H*-pyrazolo[3,4-*b*]pyridin-1-yl)-2-((*trans*-4-hydroxycyclohexyl)amino)benzamide (15a). To a solution of **31a** (20 mg, 0.045 mmol), DMSO (0.1 mL), and EtOH (0.2 mL), 4 M NaOH aq. (34 μ L, 0.14 mmol), and 30% H_2O_2 aq. (15.4 μ L, 0.14 mmol) were added on ice. After being stirred for 30 min at 0 $^\circ$ C, the reaction

mixture was allowed to warm to room temperature and stirred for 2 h. The reaction mixture was quenched with 10% Na₂S₂O₃ aq. (0.2 mL) on ice, and then diluted with CHCl₃. The mixture was extracted with CHCl₃. The organic layer was washed with 5% NaCl aq., dried over MgSO₄, and concentrated *in vacuo*. The residue was purified by column chromatography (eluent, 12%–100% EtOAc in hexane and 0%–20% MeOH in EtOAc) to obtain 19 mg (91%) of **15a** as a white powder. UPLC-MS (ESI) *m/z*=460.2 [M+H]⁺, *t_R*=1.06 min. UPLC purity 99.29%. ¹H NMR (400 MHz, DMSO-*d*₆) δ 1.08 (d, *J*=6.6 Hz, 6H), 1.19–1.38 (m, 4H), 1.79–1.97 (m, 2H), 2.02–2.14 (m, 2H), 2.98–3.17 (m, 1H), 3.24–3.33 (m, 1H), 3.45–3.53 (m, 1H), 4.58 (d, *J*=4.4 Hz, 1H), 7.15 (brs, 1H), 7.23 (s, 1H), 7.38–7.42 (m, 2H), 7.74–7.79 (m, 3H), 7.84 (brs, 1H), 8.19 (brs, 1H), 8.40 (d, *J*=7.0 Hz, 1H), 8.74 (d, *J*=4.8 Hz, 1H). HRMS calcd for C₂₅H₂₉N₇O₂ 460.2456 [M+H]⁺, found 460.2459.

The following compounds (**15b**, **15c**, **15d**, **15e**, **15f**, **15g**, **15h**, **15i**, **15j**, **15k**) were prepared from **29** and the corresponding imidazoles by a method similar to that described for **15a**.

2-((*trans*-4-hydroxycyclohexyl)amino)-4-(3-isopropyl-4-(4-phenyl-1*H*-imidazol-1-yl)-1*H*-pyrazolo[3,4-*b*]pyridin-1-yl)benzamide (15b). Yield 73% (2 steps), white powder. UPLC-MS (ESI) *m/z*=536.2 [M+H]⁺, *t_R*=1.65 min. UPLC purity 96.50%. ¹H NMR (400 MHz, DMSO-*d*₆) δ 1.13 (d, *J*=6.6 Hz, 6H), 1.20–1.39 (m, 4H), 1.83–1.91 (m, 2H), 2.05–2.14 (m, 2H), 3.15–3.24 (m, 1H), 3.24–3.36 (m, 1H), 3.45–3.54 (m, 1H), 4.58 (d, *J*=4.4 Hz, 1H), 7.15 (brs, 1H), 7.24–7.30 (m, 1H), 7.39–7.47 (m, 3H), 7.49 (d, *J*=4.8 Hz, 1H), 7.75–7.93 (m, 5H), 8.27 (s, 2H), 8.38–8.46 (m, 1H), 8.78 (d, *J*=4.8 Hz, 1H). HRMS calcd for C₃₁H₃₃N₇O₂ 536.2774 [M+H]⁺, found 536.2776.

2-((*trans*-4-hydroxycyclohexyl)amino)-4-(3-isopropyl-4-(4-(4-methoxyphenyl)-1*H*-imidazol-1-yl)-1*H*-pyrazolo[3,4-*b*]pyridin-1-yl)benzamide (15c). Yield 58% (2 steps), white powder. UPLC-MS (ESI) $m/z=566.4$ $[M+H]^+$, $t_R=1.59$ min. UPLC purity 96.56%. 1H NMR (400 MHz, DMSO- d_6) δ 1.12 (d, $J=7.0$ Hz, 6H), 1.19–1.40 (m, 4H), 1.81–1.93 (m, 2H), 2.02–2.16 (m, 2H), 3.21 (spt, $J=6.8$ Hz, 1 H), 3.25–3.35 (m, 1H), 3.44–3.55 (m, 1H), 3.77 (s, 3H), 4.59 (d, $J=4.4$ Hz, 1H), 6.96–7.01 (m, 2H), 7.16 (brs, 1H), 7.42 (dd, $J=8.8, 1.8$ Hz, 1H), 7.46 (d, $J=4.8$ Hz, 1H), 7.74–7.95 (m, 5H), 8.12–8.15 (m, 1H), 8.23 (d, $J=1.1$ Hz, 1H), 8.41 (d, $J=7.3$ Hz, 1H), 8.76 (d, $J=4.8$ Hz, 1H). HRMS calcd for $C_{32}H_{35}N_7O_3$ 566.2889 $[M+H]^+$, found 566.2889.

2-((*trans*-4-Hydroxycyclohexyl)amino)-4-(3-isopropyl-4-(4-(4-phenoxyphenyl)-1*H*-imidazol-1-yl)-1*H*-pyrazolo[3,4-*b*]pyridin-1-yl)benzamide (15d). Yield 51% (2 steps), white powder. UPLC-MS (ESI) $m/z=628.3$ $[M+H]^+$, $t_R=1.94$ min. UPLC purity 99.86%. 1H NMR (400 MHz, DMSO- d_6) δ 1.13 (d, $J=7.0$ Hz, 6H), 1.19–1.40 (m, 4H), 1.81–1.92 (m, 2H), 2.03–2.14 (m, 2H), 3.16–3.25 (m, 1H), 3.21 (spt, $J=6.8$ Hz, 1H), 3.25–3.35 (m, 1H), 3.45–3.55 (m, 1H), 4.59 (d, $J=4.4$ Hz, 1H), 7.01–7.28 (m, 6H), 7.36–7.45 (m, 3H), 7.47 (d, $J=5.1$ Hz, 1H), 7.75–7.94 (m, 5H), 8.20–8.28 (m, 2H), 8.42 (d, $J=7.0$ Hz, 1H), 8.77 (d, $J=5.1$ Hz, 1H). HRMS calcd for $C_{37}H_{37}N_7O_3$ 628.3031 $[M+H]^+$, found 628.3031.

2-((*trans*-4-hydroxycyclohexyl)amino)-4-(3-isopropyl-4-(4-(pyridin-3-yl)-1*H*-imidazol-1-yl)-1*H*-pyrazolo[3,4-*b*]pyridin-1-yl)benzamide (15e). Yield 50% (2 steps), white powder. UPLC-MS (ESI) $m/z=537.2$ $[M+H]^+$, $t_R=1.15$ min. UPLC purity 99.09%. 1H NMR (400 MHz, DMSO- d_6) δ 1.13 (d, $J=6.6$ Hz, 6H), 1.21–1.42 (m, 4H), 1.74–1.93 (m, 2H), 2.02–2.16 (m, 2H), 3.18 (spt, $J=6.8$ Hz, 1H), 3.25–3.36 (m, 1H), 3.44–3.54 (m, 1H), 4.58 (d, $J=4.4$ Hz, 1H), 7.16 (brs, 1H), 7.40–7.48 (m, 2H), 7.50 (d, $J=4.8$ Hz, 1H), 7.75–7.81 (m, 2H), 7.85 (brs, 1H), 8.22 (dt,

$J=8.0$, 1.9 Hz, $1H$), 8.35 – 8.49 (m, $4H$), 8.79 (d, $J=5.1$ Hz, $1H$), 9.10 (s, $1H$). HRMS calcd for $C_{30}H_{32}N_8O_2$ 537.2726 $[M+H]^+$, found 537.2733 .

2-((*trans*-4-hydroxycyclohexyl)amino)-4-(3-isopropyl-4-(4-(pyridin-4-yl)-1*H*-imidazol-1-yl)-1*H*-pyrazolo[3,4-*b*]pyridin-1-yl)benzamide (15f). Yield 41% (2 steps), white powder. UPLC-MS (ESI) $m/z=537.1$ $[M+H]^+$, $t_R=1.22$ min. UPLC purity 99.85%. 1H NMR (400 MHz, $DMSO-d_6$) δ 1.11 (d, $J=7.0$ Hz, $6H$), 1.20–1.39 (m, $4H$), 1.81–1.92 (m, $2H$), 2.05–2.14 (m, $2H$), 3.14 (spt, $J=6.8$ Hz, $1H$), 3.10–3.18 (m, $1H$), 3.26–3.35 (m, $1H$), 3.45–3.55 (m, $1H$), 4.59 (d, $J=4.4$ Hz, $1H$), 7.16 (brs, $1H$), 7.42 (dd, $J=8.6$, 2.0 Hz, $1H$), 7.51 (d, $J=4.8$ Hz, $1H$), 7.76–7.90 (m, $5H$), 8.34–8.46 (m, $2H$), 8.55–8.62 (m, $3H$), 8.80 (d, $J=4.8$ Hz, $1H$). HRMS calcd for $C_{30}H_{32}N_8O_2$ 537.2721 $[M+H]^+$, found 537.2724 .

2-((*trans*-4-hydroxycyclohexyl)amino)-4-(3-isopropyl-4-(4-(pyrimidin-5-yl)-1*H*-imidazol-1-yl)-1*H*-pyrazolo[3,4-*b*]pyridin-1-yl)benzamide (15g). Yield 50% (2 steps), white powder. UPLC-MS (ESI) $m/z=538.2$ $[M+H]^+$, $t_R=1.30$ min. UPLC purity 97.94%. 1H NMR (400 MHz, $DMSO-d_6$) δ 1.12 (d, $J=6.6$ Hz, $6H$), 1.17–1.41 (m, $4H$), 1.81–1.93 (m, $2H$), 2.01–2.17 (m, $2H$), 3.16 (spt, $J=6.8$ Hz, $1H$), 3.24–3.36 (m, $1H$), 3.45–3.54 (m, $1H$), 4.59 (d, $J=4.4$ Hz, $1H$), 7.17 (brs, $1H$), 7.41 (dd, $J=8.6$, 2.0 Hz, $1H$), 7.51 (d, $J=4.8$ Hz, $1H$), 7.78 (dd, $J=5.3$, 3.5 Hz, $2H$), 7.86 (brs, $1H$), 8.39–8.46 (m, $2H$), 8.54 (s, $1H$), 8.80 (d, $J=5.1$ Hz, $1H$), 9.10 (s, $1H$), 9.26 (s, $2H$). HRMS calcd for $C_{29}H_{31}N_9O_2$ 538.2679 $[M+H]^+$, found 538.2686 .

4-(4-(4-(furan-3-yl)-1*H*-imidazol-1-yl)-3-isopropyl-1*H*-pyrazolo[3,4-*b*]pyridin-1-yl)-2-((*trans*-4-hydroxycyclohexyl)amino)benzamide (15h). Yield 23% (2 steps), white powder. UPLC-MS (ESI) $m/z=526.1$ $[M+H]^+$, $t_R=1.50$ min. UPLC purity 96.27%. 1H NMR (400 MHz, $CDCl_3$) δ 1.25 (d, $J=6.6$ Hz, $6H$), 1.38–1.61 (m, $4H$), 2.03–2.12 (m, $2H$), 2.23–2.31 (m, $2H$),

3.13 (spt, $J=6.8$ Hz, 1H), 3.40–3.55 (m, 1H), 3.55–3.66 (m, 1H), 3.73–3.81 (m, 1H), 5.62 (brs, 2H), 6.72 (d, $J=1.5$ Hz, 1H), 7.15 (d, $J=4.8$ Hz, 1H), 7.37 (d, $J=1.1$ Hz, 1H), 7.49–7.54 (m, 3H), 7.83 (d, $J=1.5$ Hz, 1H), 7.89–7.95 (m, 2H), 8.08 (brd, $J=7.3$ Hz, 1H), 8.68 (d, $J=4.8$ Hz, 1H). HRMS calcd for $C_{29}H_{31}N_7O_3$ 526.2561 $[M+H]^+$, found 526.2558.

2-((*trans*-4-hydroxycyclohexyl)amino)-4-(3-isopropyl-4-(4-(thiophen-3-yl)-1*H*-imidazol-1-yl)-1*H*-pyrazolo[3,4-*b*]pyridin-1-yl)benzamide (15i). Yield 40% (2 steps), white powder. UPLC-MS (ESI) $m/z=542.1$ $[M+H]^+$, $t_R=1.58$ min. UPLC purity 95.41%. 1H NMR (400 MHz, $CDCl_3$) δ 1.25 (d, $J=6.6$ Hz, 6H), 1.38–1.63 (m, 4H), 1.98–2.18 (m, 2H), 2.21–2.32 (m, 2H), 3.14 (spt, $J=6.7$ Hz, 1H), 3.38–3.60 (m, 1H), 3.63–3.81 (m, 1H), 5.63 (brs, 2H), 7.14–7.18 (m, 1H), 7.16 (d, $J=4.8$ Hz, 1H), 7.39–7.57 (m, 5H), 7.72 (d, $J=2.2$ Hz, 1H), 7.84 (s, 1H), 7.91 (s, 1H), 8.08 (brd, $J=6.6$ Hz, 1H), 8.68 (d, $J=5.1$ Hz, 1H). HRMS calcd for $C_{29}H_{31}N_7O_2S$ 542.2333 $[M+H]^+$, found 542.2333.

4-(4-(1'*H*-[1,4'-biimidazol]-1'-yl)-3-isopropyl-1*H*-pyrazolo[3,4-*b*]pyridin-1-yl)-2-((*trans*-4-hydroxycyclohexyl)amino)benzamide (15j). Yield 52% (2 steps), white powder. UPLC-MS (ESI) $m/z=526.2$ $[M+H]^+$, $t_R=1.07$ min. UPLC purity 98.39%. 1H NMR (400 MHz, $DMSO-d_6$) δ 1.14 (d, $J=7.0$ Hz, 6H), 1.20–1.39 (m, 4H), 1.79–1.95 (m, 2H), 2.03–2.15 (m, 2H), 3.13–3.22 (m, 1H), 3.25–3.35 (m, 1H), 3.45–3.55 (m, 1H), 4.59 (d, $J=4.0$ Hz, 1H), 7.10 (brs, 1H), 7.17 (brs, 1H), 7.41 (dd, $J=8.6, 2.0$ Hz, 1H), 7.51 (d, $J=4.8$ Hz, 1H), 7.67 (s, 1H), 7.75–7.82 (m, 2H), 7.86 (brs, 1H), 8.11 (d, $J=1.5$ Hz, 1H), 8.20 (brs, 1H), 8.30 (d, $J=1.5$ Hz, 1H), 8.41 (d, $J=7.3$ Hz, 1H), 8.80 (d, $J=4.8$ Hz, 1H). HRMS calcd for $C_{28}H_{31}N_9O_2$ 526.2674 $[M+H]^+$, found 526.2681.

2-((*trans*-4-hydroxycyclohexyl)amino)-4-(3-isopropyl-4-(4-(1-methyl-1*H*-pyrazol-4-yl)-1*H*-imidazol-1-yl)-1*H*-pyrazolo[3,4-*b*]pyridin-1-yl)benzamide (15k). Yield 41% (2 steps), white

powder. UPLC-MS (ESI) $m/z=540.4$ $[M+H]^+$, $t_R=1.29$ min. UPLC purity 96.57%. 1H NMR (400 MHz, DMSO- d_6) δ 1.12 (d, $J=6.6$ Hz, 6H), 1.17–1.41 (m, 4H), 1.71–1.94 (m, 2H), 2.03–2.14 (m, 2H), 3.19 (spt, $J=6.8$ Hz, 1H), 3.25–3.34 (m, 1H), 3.45–3.54 (m, 1H), 3.86 (s, 3H), 4.58 (d, $J=4.4$ Hz, 1H), 7.15 (brs, 1H), 7.39–7.46 (m, 2H), 7.70–7.89 (m, 5H), 7.97 (s, 1H), 8.18 (d, $J=1.1$ Hz, 1H), 8.41 (d, $J=7.0$ Hz, 1H), 8.75 (d, $J=4.8$ Hz, 1H). HRMS calcd for $C_{29}H_{33}N_9O_2$ 540.2830 $[M+H]^+$, found 540.2833.

4-(3-Isopropyl-4-(4-(1-methyl-1*H*-pyrazol-4-yl)-1*H*-imidazol-1-yl)-1*H*-pyrazolo[3,4-*b*]pyridin-1-yl)benzamide (16a). To a solution of **36a** (4.5 mg, 0.011 mmol), DMSO (45 μ L), and EtOH (90 μ L), 4 M NaOH aq. (2.8 μ L, 0.011 mmol) and 30% H_2O_2 aq. (3.7 μ L, 0.033 mmol) were added under ice cooling. After being stirred for 30 min at 0 $^\circ$ C, the reaction mixture was allowed to warm to room temperature and stirred for 4 h. The reaction mixture was quenched with 10% aqueous $Na_2S_2O_3$ (45 μ L) under ice cooling, and then diluted with $CHCl_3$. The mixture was extracted with $CHCl_3$. The organic layer was washed with 5% aqueous NaCl, dried over $MgSO_4$, and concentrated in vacuo. The residue was purified by column chromatography (eluent, 0%–20% MeOH in EtOAc) to obtain 4.1 mg (87%) of **16a** as a white powder. UPLC-MS (ESI) $m/z=427.1$ $[M+H]^+$, $t_R=1.18$ min. UPLC purity 96.04%. 1H NMR (400 MHz, DMSO- d_6) δ 1.13 (d, $J=6.6$ Hz, 6H), 3.19 (spt, $J=6.8$ Hz, 1H), 3.86 (s, 3H), 7.42 (brs, 1H), 7.47 (d, $J=5.1$ Hz, 1H), 7.73 (s, 1H), 7.87 (d, $J=1.5$ Hz, 1H), 7.97 (s, 1H), 8.02–8.12 (m, 3H), 8.18 (d, $J=1.1$ Hz, 1H), 8.37–8.42 (m, 2H), 8.79 (d, $J=4.8$ Hz, 1H). HRMS calcd for $C_{23}H_{22}N_8O$ 427.1989 $[M+H]^+$, found 427.1997.

The following compounds (**16b**) were prepared from **36b** by a method similar to that described for **16a**.

**4-(3-Isopropyl-4-(4-(1-methyl-1*H*-pyrazol-4-yl)-1*H*-imidazol-1-yl)-1*H*-pyrazolo[3,4-
b]pyridin-1-yl)-2-(methylamino)benzamide (16b).** Yield 45%, white powder. UPLC-MS (ESI)
 $m/z=456.1$ $[M+H]^+$, $t_R=1.30$ min. UPLC purity 98.71%. 1H NMR (400 MHz, DMSO- d_6) δ 1.12
(d, $J=6.6$ Hz, 6H), 2.87 (d, $J=5.1$ Hz, 3H), 3.18 (spt, $J=6.7$ Hz, 1H), 3.86 (s, 3H), 7.21 (brs, 1H),
7.43 (d, $J=5.1$ Hz, 1H), 7.48 (dd, $J=8.6, 2.0$ Hz, 1H), 7.64 (d, $J=2.2$ Hz, 1H), 7.73 (s, 1H), 7.79
(d, $J=8.4$ Hz, 1H), 7.82–7.92 (m, 2H), 7.97 (s, 1H), 8.18 (d, $J=1.1$ Hz, 1H), 8.31 (q, $J=4.8$ Hz,
1H), 8.77 (d, $J=4.8$ Hz, 1H). HRMS calcd for $C_{24}H_{25}N_9O$ 456.2255 $[M+H]^+$, found 456.2256.

**4-(3-Isopropyl-4-(4-(1-methyl-1*H*-pyrazol-4-yl)-1*H*-imidazol-1-yl)-1*H*-pyrazolo[3,4-
b]pyridin-1-yl)-3-(methylamino)benzamide (16c).** To a solution of **39** (18.9 mg, 0.043 mmol),
DMSO (95 μ L), and EtOH (189 μ L), 4 M NaOH aq. (5.4 μ L, 0.022 mmol), and 30% H_2O_2 aq.
(14.7 μ L, 0.13 mmol) were added on ice. After being stirred for 2 h at 0 °C, the reaction mixture
was quenched with 10% $Na_2S_2O_3$ aq. (189 μ L) on ice, and then diluted with AcOEt. The mixture
was extracted with AcOEt. The organic layer was washed with 5% NaCl aq., dried over $MgSO_4$,
and concentrated *in vacuo*. The residue was purified by column chromatography (eluent, 0%–
20% MeOH in EtOAc) to obtain 18.8 mg (96%) of **16c** as a white powder. UPLC-MS (ESI)
 $m/z=456.1$ $[M+H]^+$, $t_R=1.10$ min. UPLC purity 97.36%. 1H NMR (400 MHz, $CDCl_3$) δ 1.25 (d,
 $J=7.0$ Hz, 6H), 2.94 (d, $J=4.8$ Hz, 3H), 3.18 (spt, $J=6.8$ Hz, 1H), 3.98 (s, 3H), 5.33–5.44 (m, 1H),
5.64 (brs, 1H), 6.13 (brs, 1H), 7.15 (d, $J=4.8$ Hz, 1H), 7.20 (dd, $J=8.1, 1.8$ Hz, 1H), 7.36 (d,
 $J=1.5$ Hz, 1H), 7.40 (d, $J=1.8$ Hz, 1H), 7.65 (d, $J=8.1$ Hz, 1H), 7.80 (d, $J=1.5$ Hz, 2H), 7.83 (d,
 $J=1.1$ Hz, 1H), 8.65 (d, $J=4.8$ Hz, 1H). HRMS calcd for $C_{24}H_{25}N_9O$ 456.2260 $[M+H]^+$, found
456.2253.

The following compounds (**16d**, **16e**) were prepared from **37** and the corresponding benzonitriles by a method similar to that described for **16a**.

4-(3-Isopropyl-4-(4-(1-methyl-1*H*-pyrazol-4-yl)-1*H*-imidazol-1-yl)-1*H*-pyrazolo[3,4-*b*]pyridin-1-yl)-3-methylbenzamide (16d). Yield 85% (2 steps), white powder. UPLC-MS (ESI) $m/z=441.3$ $[M+H]^+$, $t_R=1.12$ min. UPLC purity 98.85%. 1H NMR (400 MHz, DMSO- d_6) δ 1.10 (d, $J=6.6$ Hz, 6H), 2.17 (s, 3H), 3.17–3.25 (m, 1H), 3.86 (s, 3H), 7.39 (d, $J=5.1$ Hz, 1H), 7.48 (s, 1H), 7.53 (d, $J=8.1$ Hz, 1H), 7.73 (s, 1H), 7.86 (dd, $J=8.1, 1.8$ Hz, 1H), 7.89 (d, $J=1.1$ Hz, 1H), 7.95–7.98 (m, 2H), 8.08 (s, 1H), 8.19 (d, $J=1.1$ Hz, 1H), 8.63 (d, $J=4.8$ Hz, 1H). HRMS calcd for $C_{24}H_{24}N_8O$ 441.2151 $[M+H]^+$, found 441.2152.

3-Ethyl-4-(3-isopropyl-4-(4-(1-methyl-1*H*-pyrazol-4-yl)-1*H*-imidazol-1-yl)-1*H*-pyrazolo[3,4-*b*]pyridin-1-yl)benzamide (16e). Yield 64% (2 steps), white powder. UPLC-MS (ESI) $m/z=454.8$ $[M+H]^+$, $t_R=1.19$ min. UPLC purity 99.65%. 1H NMR (400 MHz, $CDCl_3$) δ 1.14 (t, $J=7.5$ Hz, 3H), 1.25 (d, $J=7.0$ Hz, 6H), 2.62 (q, $J=7.3$ Hz, 2H), 3.18 (spt, $J=6.8$ Hz, 1H), 3.98 (s, 3H), 5.88 (brs, 1H), 6.22 (brs, 1H), 7.13 (d, $J=5.1$ Hz, 1H), 7.39 (d, $J=1.1$ Hz, 1H), 7.58 (d, $J=8.1$ Hz, 1H), 7.78–7.81 (m, 3H), 7.86 (d, $J=1.5$ Hz, 1H), 7.96 (d, $J=1.8$ Hz, 1H), 8.59 (d, $J=4.7$ Hz, 1H). HRMS calcd for $C_{25}H_{26}N_8O$ 455.2308 $[M+H]^+$, found 455.2311.

3-(1*H*-Indol-4-yl)quinoline (18a). The mixture of 4-bromoindole (**17a**, 3.0 g, 15.3 mmol), 3-quinoline boronic acid (2.78 g, 16.1 mmol), $Pd(PPh_3)_4$ (0.884 g, 0.77 mmol), and Na_2CO_3 (3.41 g, 32.1 mmol) in DME (30 mL) and H_2O (30 mL) was stirred at 100 °C for 14 h under nitrogen atmosphere. After cooling to room temperature, the reaction mixture was concentrated *in vacuo*. The residue was extracted with $CHCl_3$. The organic layer was dried over $MgSO_4$ and concentrated *in vacuo*. The residue was purified by column chromatography (eluent, 0%–15%

MeOH in CHCl_3) to obtain 1.87 g (50%) of **18a** as a yellow oil. UPLC-MS (ESI) $m/z=244.8$ $[\text{M}+\text{H}]^+$, $t_R=1.35$ min. ^1H NMR (400 MHz, CDCl_3) δ 6.76–6.79 (m, 1H), 7.30–7.38 (m, 3H), 7.48–7.52 (m, 1H), 7.56–7.64 (m, 1H), 7.70–7.79 (m, 1H), 7.91 (d, $J=8.1$ Hz, 1H), 8.18 (d, $J=8.4$ Hz, 1H), 8.39–8.52 (m, 2 H), 9.31 (d, $J=2.2$ Hz, 1H).

2-((*trans*-4-Hydroxycyclohexyl)amino)-4-(4-(quinolin-3-yl)-1*H*-indol-1-yl)benzonitrile

(20a). The mixture of **18a** (100 mg, 0.409 mmol), **19** (154 mg, 0.45 mmol), CuI (7.8 mg, 0.041 mmol), DMEDA (8.8 μL , 0.082 mmol), Cs_2CO_3 (267 mg, 0.82 mmol), and 1,4-dioxane (1 mL) was stirred at 110 $^\circ\text{C}$ for 14 h under nitrogen atmosphere. After cooling to room temperature, the reaction mixture was diluted with EtOAc and filtered through a pad of celite. The celite pad was washed with EtOAc and the filtrate was concentrated *in vacuo*. The residue was purified by column chromatography (eluent, 12%–100% EtOAc in hexane) to obtain 178 mg (95%) of **20a** as a pale-yellow powder. UPLC-MS (ESI) $m/z=459.4$ $[\text{M}+\text{H}]^+$, $t_R=1.86$ min. ^1H NMR (400 MHz, CDCl_3) δ 1.34–1.52 (m, 4H), 2.02–2.23 (m, 4H), 3.33–3.45 (m, 1H), 3.66–3.80 (m, 1H), 4.61 (d, $J=7.6$ Hz, 1H), 6.78–6.93 (m, 3H), 7.38–7.47 (m, 3H), 7.53–7.71 (m, 3H), 7.74–7.81 (m, 1H), 7.94 (d, $J=8.1$ Hz, 1H), 8.21 (d, $J=8.3$ Hz, 1H), 8.44 (d, $J=1.7$ Hz, 1H), 9.30 (brs, 1H).

3-(1*H*-Indazol-4-yl)quinoline (22a). The mixture of **21a** (100 mg, 0.51 mmol), 3-quinoline boronic acid (141 mg, 0.81 mmol), $\text{Pd}(\text{dppf})\text{Cl}_2 \cdot \text{CH}_2\text{Cl}_2$ (41.5 mg, 0.051 mmol), and Na_2CO_3 (108 mg, 1.02 mmol) in 1,4-dioxane (2 mL) and H_2O (1 mL) was stirred at 100 $^\circ\text{C}$ for 3 h. After cooling to room temperature, the reaction mixture was diluted with water and EtOAc. The organic layer was washed with brine, dried over Na_2SO_4 , and concentrated *in vacuo*. The residue was purified by column chromatography (eluent, 12%–100% EtOAc in hexane) to obtain 117 mg (94%) of **22a** as a yellow amorphous solid. UPLC-MS (ESI) $m/z=246.2$ $[\text{M}+\text{H}]^+$, $t_R=1.26$

min. ^1H NMR (400 MHz, CDCl_3) δ 7.39 (dd, $J=6.7, 1.1$ Hz, 1H), 7.52–7.66 (m, 3H), 7.74–7.83 (m, 1H), 7.91–7.97 (m, 1H), 8.21 (d, $J=8.29$ Hz, 1H), 8.30 (d, $J=1.0$ Hz, 1H), 8.47 (d, $J=2.2$ Hz, 1H), 9.31 (d, $J=2.4$ Hz, 1H), 10.59 (brs, 1H).

2-((*trans*-4-Hydroxycyclohexyl)amino)-4-(4-(quinolin-3-yl)-1*H*-indazol-1-yl)benzonitrile

(23a). The mixture of **22a** (30 mg, 0.12 mmol), **19** (46 mg, 0.14 mmol), CuI (2.3 mg, 0.012 mmol), DMEDA (2.6 μL , 0.025 mmol), K_3PO_4 (54.5 mg, 0.26 mmol), and 1,4-dioxane (0.3 mL) was stirred at 110 $^\circ\text{C}$ for 24 h. After cooling to room temperature, the reaction mixture was diluted with EtOAc and filtered through a pad of celite. The celite pad was washed with EtOAc and the filtrate was concentrated *in vacuo*. The residue was purified by column chromatography (eluent, 12%–100% EtOAc in hexane) to obtain 55 mg (98%) of **23a** as a pale-yellow powder. UPLC-MS (ESI) $m/z=460.1$ $[\text{M}+\text{H}]^+$, $t_R=1.78$ min. ^1H NMR (400 MHz, CDCl_3) δ 1.35–1.54 (m, 4H), 2.01–2.13 (m, 2H), 2.21 (m, 2H), 3.41–3.56 (m, 1H), 3.69–3.79 (m, 1H), 4.59 (d, $J=7.8$ Hz, 1H), 7.07–7.15 (m, 2H), 7.47 (d, $J=7.1$ Hz, 1H), 7.56–7.69 (m, 2H), 7.79–7.83 (m, 1H), 7.85 (d, $J=8.5$ Hz, 1H), 7.96 (d, $J=7.8$ Hz, 1H), 8.22 (d, $J=8.5$ Hz, 1H), 8.37–8.41 (m, 1H), 8.46 (d, $J=2.0$ Hz, 1H), 9.29 (d, $J=2.0$ Hz, 1H).

4-Chloro-3-isopropyl-1*H*-pyrazolo[4,3-*c*]pyridine (25a). To a solution of DIPA (2.09 mL, 14.9 mmol) in THF (20 mL), *n*BuLi solution (1.58 M in hexane, 5.70 mL, 14.9 mmol) was added dropwise at 0 $^\circ\text{C}$, and the mixture was stirred for 10 min. To a solution of 2,4-dichloropyridine **24a** (2.0 g, 13.5 mmol) in THF (20 mL), LDA solution prepared as mentioned above was added dropwise at -78 $^\circ\text{C}$. The reaction mixture was stirred for 15 min at that temperature, and then isobutylaldehyde (2.36 mL, 14.2 mmol) was added. After being stirred for 1 h at -78 $^\circ\text{C}$, the reaction mixture was allowed to warm to room temperature. To the reaction mixture, hydrazine monohydrate (1.35 mL, 27.0 mmol) was added and stirred at 70 $^\circ\text{C}$ for 24 h. After cooling to

room temperature, the reaction mixture was quenched with water and the organic materials were extracted with EtOAc. The combined organic phases were washed with brine and dried over Na_2SO_4 . The organic phase was concentrated *in vacuo* and the residue was purified by silica gel column chromatography (eluent, 12%–100% EtOAc in hexane and 0%–20% MeOH in EtOAc) to obtain 642 mg (24%) of **25a** and its regioisomer (186 mg, 7%) as a white powder. UPLC-MS (ESI) m/z =196.1, 197.8 $[\text{M}+\text{H}]^+$, t_R =1.36 min. ^1H NMR (400 MHz, CDCl_3) δ 1.37–1.55 (m, 6H), 3.78–3.91 (m, 1H), 8.13–8.28 (m, 1H), 10.13–10.39 (m, 1H).

3-(3-Isopropyl-1H-pyrazolo[4,3-c]pyridin-4-yl)quinoline (26a). The mixture of **25a** (539 mg, 2.76 mmol), 3-quinoline boronic acid (763 mg, 4.41 mmol), $\text{Pd}(\text{dppf})\text{Cl}_2\cdot\text{CH}_2\text{Cl}_2$ (225 mg, 0.28 mmol), and Na_2CO_3 (584 mg, 5.51 mmol) in 1,4-dioxane (10.8 mL) and H_2O (5.4 mL) was stirred at 100 °C for 3 h. After cooling to room temperature, the reaction mixture was diluted with water and EtOAc. The organic layer was washed with brine, dried over Na_2SO_4 , and concentrated *in vacuo*. The residue was purified by column chromatography (eluent, 12%–100% EtOAc in hexane and 0%–20% MeOH in EtOAc) to obtain 732 mg (92%) of **26a** as a yellow powder. UPLC-MS (ESI) m/z =289.3 $[\text{M}+\text{H}]^+$, t_R =1.03 min. ^1H NMR (400 MHz, CDCl_3) δ 1.13 (d, J =7.0 Hz, 6H), 3.04–3.13 (m, 1H), 7.41 (d, J =5.9 Hz, 1H), 7.62–7.67 (m, 1H), 7.79–7.84 (m, 1H), 7.93 (d, J =8.1 Hz, 1H), 8.23 (d, J =8.8 Hz, 1H), 8.46 (d, J =1.5 Hz, 1H), 8.54 (d, J =6.2 Hz, 1H), 9.20 (d, J =2.2 Hz, 1H), 10.35 (brs, 1H).

2-((trans-4-Hydroxycyclohexyl)amino)-4-(3-isopropyl-4-(quinolin-3-yl)-1H-pyrazolo[4,3-c]pyridin-1-yl)benzonitrile (27a). The mixture of **26a** (200 mg, 0.69 mmol), **19** (261 mg, 0.76 mmol), CuI (13.2 mg, 0.069 mmol), DMEDA (14.9 μL , 0.139 mmol), K_3PO_4 (309 mg, 1.46 mmol), and 1,4-dioxane (2 mL) was stirred at 110 °C for 24 h. After cooling to room temperature, the reaction mixture was diluted with EtOAc and filtered through a pad of celite.

The celite pad was washed with EtOAc and the filtrate was concentrated *in vacuo*. The residue was purified by column chromatography (eluent, 12%–100% EtOAc in hexane) to obtain 283 mg (81%) of **27a** as a pale-yellow powder. UPLC-MS (ESI) $m/z=503.3$ $[M+H]^+$, $t_R=1.66$ min. 1H NMR (400 MHz, $CDCl_3$) δ 1.16 (d, $J=7.0$ Hz, 6H), 1.33–1.55 (m, 4H), 2.02–2.11 (m, 2H), 2.17–2.23 (m, 2H), 3.09 (spt, $J=6.8$ Hz, 1H), 3.40–3.49 (m, 1H), 3.71–3.78 (m, 1H), 4.61 (d, $J=7.3$ Hz, 1H), 7.04–7.08 (m, 2H), 7.57 (d, $J=8.1$ Hz, 1H), 7.63–7.68 (m, 2H), 7.81–7.86 (m, 1H), 7.95 (d, $J=7.3$ Hz, 1H), 8.23 (d, $J=8.4$ Hz, 1H), 8.46 (d, $J=2.2$ Hz, 1H), 8.62 (d, $J=5.9$ Hz, 1H), 9.19 (d, $J=2.2$ Hz, 1H).

2-Fluoro-4-(4-iodo-3-isopropyl-1H-pyrazolo[3,4-*b*]pyridin-1-yl)benzonitrile (28). To a solution of **25c** (10.0 g, 34.8 mmol) in DMF (100 mL), NaH (50%, 1.84 g, 38.3 mmol) was added at 0 °C under nitrogen atmosphere. After being stirred for 10 min at 0 °C, to the reaction mixture, 2,4-difluoro-benzonitrile (5.33 g, 38.3 mmol) was added at the same temperature. Subsequently, the reaction mixture was stirred at 60 °C for 1 h. Water was added to the mixture, and the mixture was stirred at room temperature for 1 h. The resulting precipitate was collected by filtration. The precipitate was washed with water and dried under vacuum to obtain a mixture of 13.4 g (95%) of **28** and its regioisomer **28a** as a white powder. The crude product was used for the next reaction without further purification.

2-((*trans*-4-Hydroxycyclohexyl)amino)-4-(4-iodo-3-isopropyl-1H-pyrazolo[3,4-*b*]pyridin-1-yl)benzonitrile (29). The solution of **29** (13.4 g, 33.1 mmol), *trans*-4-aminocyclohexanol (4.19 g, 36.4 mmol), DIPEA (5.76 mL, 33.1 mmol), and DMSO (81 mL) was stirred at 125 °C for 5 h under nitrogen atmosphere. Subsequently, the reaction was warmed to 150 °C and stirred for 3 h. Water (241 mL) was added to the mixture, and the mixture was stirred at room temperature for 2 h. The resulting precipitate was collected by filtration. The precipitate was washed with water

and dried under vacuum to obtain crude **29** as a brown amorphous solid. The crude **29** was purified by column chromatography (eluent, 12%–100% EtOAc in hexane) to obtain 2.50 g (15%) of **29** as a pale-red powder. UPLC-MS (ESI) $m/z=501.9$ $[M+H]^+$, $t_R=2.40$ min. 1H NMR (400 MHz, DMSO- d_6) δ 1.26–1.43 (m, 4H), 1.45 (d, $J=6.8$ Hz, 6H), 1.83–1.93 (m, 2H), 1.96–2.05 (m, 2H), 3.33–3.48 (m, 2H), 3.93 (spt, $J=6.8$ Hz, 1H), 4.59 (brs, 1H), 5.81–5.89 (m, 1H), 7.56–7.64 (m, 2H), 7.87–7.95 (m, 2H), 8.19–8.24 (m, 1H).

2-((trans-4-Hydroxycyclohexyl)amino)-4-(3-isopropyl-4-(naphthalen-2-yl)-1H-pyrazolo[3,4-*b*]pyridin-1-yl)benzonitrile (30a). The mixture of **29** (50 mg, 0.10 mmol), 3-quinoline boronic acid (21 mg, 0.12 mmol), $Pd(PPh_3)_4$ (5.8 mg, 0.005 mmol), and Na_2CO_3 (12.7 mg, 0.12 mmol) in DME (1.0 mL) and H_2O (0.5 mL) was stirred at 100 °C for 4 h under nitrogen atmosphere. After cooling to room temperature, the reaction mixture was quenched with 10% $NaHCO_3$ aq. The mixture was diluted with EtOAc and filtered through a pad of celite. The celite pad was washed with EtOAc, and the filtrate was washed with 5% NaCl aq. and concentrated *in vacuo*. The residue was purified by column chromatography (eluent, 12%–100% EtOAc in hexane and 0%–20% MeOH in EtOAc) to obtain 48 mg (96%) of **30a** as a pale-yellow powder. UPLC-MS (ESI) $m/z=502.4$ $[M+H]^+$, $t_R=2.53$ min. 1H NMR (400 MHz, $CDCl_3$) δ 1.10 (d, $J=6.6$ Hz, 6H), 1.32–1.45 (m, 2H), 1.46–1.52 (m, 2H), 2.00–2.19 (m, 2H), 2.19–2.38 (m, 2H), 3.01 (spt, $J=6.8$ Hz, 1H), 3.49–3.58 (m, 1H), 3.72–3.80 (m, 1H), 4.49 (d, $J=7.33$ Hz, 1H), 7.17 (d, $J=4.8$ Hz, 1H), 7.49–7.53 (m, 1H), 7.56–7.64 (m, 3H), 7.77–7.82 (m, 1H), 7.89–8.02 (m, 4H), 8.06–8.13 (m, 1H), 8.60–8.65 (m, 1H).

4-(4-(1H-imidazol-1-yl)-3-isopropyl-1H-pyrazolo[3,4-*b*]pyridin-1-yl)-2-((trans-4-hydroxycyclohexyl)amino)benzonitrile (31a). The mixture of **29** (50 mg, 0.10 mmol), imidazole (8.2 mg, 0.12 mmol), CuO (4.0 mg, 0.05 mmol), K_2CO_3 (27.6 mg, 0.20 mmol), and

DMF (0.5 mL) was stirred at 120 °C for 20 h under nitrogen atmosphere. After cooling to room temperature, the reaction mixture was diluted with EtOAc and filtered through a pad of celite. The celite pad was washed with EtOAc, and the filtrate was washed with brine, dried over MgSO₄, and concentrated *in vacuo*. The residue was purified by column chromatography (eluent, 12%–100% EtOAc in hexane and 0%–20% MeOH in EtOAc) to obtain 29 mg (66%) of **31a** as a pale-yellow powder. UPLC-MS (ESI) *m/z*=443.0 [M+H]⁺, *t_R*=1.43 min. ¹H NMR (400 MHz, CDCl₃) δ 1.19 (d, *J*=6.6 Hz, 6H), 1.32–1.57 (m, 4H), 2.03–2.13 (m, 2H), 2.21–2.30 (m, 2H), 2.95–3.07 (m, 1H), 3.45–3.55 (m, 1H), 3.72–3.80 (m, 1H), 4.52 (d, *J*=7.3 Hz, 1H), 7.14 (d, *J*=5.1 Hz, 1H), 7.27–7.41 (m, 2H), 7.51 (d, *J*=8.4 Hz, 1H), 7.72 (dd, *J*=8.4, 1.8 Hz, 1H), 7.83 (brs, 1H), 7.97 (d, *J*=1.5 Hz, 1H), 8.67 (d, *J*=4.8 Hz, 1H).

4-Iodo-3-isopropyl-1-(4-methoxybenzyl)-1H-pyrazolo[3,4-*b*]pyridine (32). To a solution of **25c** (10.0 g, 34.8 mmol) in DMF (100 mL), NaH (50%, 2.0 g, 41.8 mmol) was added at 0 °C and stirred for 10 min under nitrogen atmosphere. To the reaction mixture 5.2 mL of PMBCl (38.3 mmol) was added at 0 °C. After being stirred for 10 min at 0 °C, the reaction mixture was allowed to warm to room temperature and stirred for 2 h. The reaction mixture was quenched with water and diluted with AcOEt. The organic phase was washed with brine and dried over anhydrous MgSO₄, and concentrated *in vacuo*. The residue was purified by column chromatography (eluent, 6%–60% EtOAc in hexane) to obtain 12.8 g (91%) of **32** as a yellow oil. UPLC-MS (ESI) *m/z*=408.3 [M+H]⁺, *t_R*=2.36 min. ¹H NMR (400 MHz, CDCl₃) δ 1.43 (d, *J*=6.8 Hz, 6H), 3.74 (s, 3H), 3.89 (spt, *J*=6.8 Hz, 1H), 5.58 (s, 2H), 6.78–6.83 (m, 2H), 7.24–7.31 (m, 2H), 7.52 (d, *J*=4.9 Hz, 1H), 8.00 (d, *J*=4.9 Hz, 1H).

3-Isopropyl-1-(4-methoxybenzyl)-4-(4-(1-methyl-1H-pyrazol-4-yl)-1H-imidazol-1-yl)-1H-pyrazolo[3,4-*b*]pyridine (34). The mixture of **32** (1.0 g, 2.46 mmol), **33** (652 mg, 2.95 mmol),

Cu₂O (10.5 mg, 0.074 mmol), 4,7-dimethoxy-1,10-phenanthroline (53.1 mg, 0.221 mmol), Cs₂CO₃ (2.4 g, 7.37 mmol), PEG (491 mg), and DMSO (10 mL) was stirred at 110 °C for 24 h under nitrogen atmosphere. After cooling to room temperature, the reaction mixture was diluted with EtOAc and filtered through a pad of celite. The celite pad was washed with EtOAc, and the filtrate was diluted with water, washed with brine, dried over Na₂SO₄, and concentrated in vacuo. The residue was purified by column chromatography (eluent, 12%–100% EtOAc in hexane and 0%–20% MeOH in EtOAc) to obtain 654 mg (62%) of **34** as a pale-yellow oil. UPLC-MS (ESI) *m/z*=428.3 [M+H]⁺, *t_R*=1.53 min. ¹H NMR (400 MHz, CDCl₃) δ 1.18 (d, *J*=6.6 Hz, 6H), 3.07 (spt, *J*=6.9 Hz, 1H), 3.77 (s, 3H), 3.96 (s, 3H), 5.66 (s, 2H), 6.81–6.86 (m, 2H), 7.00 (d, *J*=5.1 Hz, 1H), 7.30 (d, *J*=1.5 Hz, 1H), 7.33–7.38 (m, 2H), 7.75–7.78 (m, 3H), 8.57 (d, *J*=4.8 Hz, 1H).

3-Isopropyl-4-(4-(1-methyl-1*H*-pyrazol-4-yl)-1*H*-imidazol-1-yl)-1*H*-pyrazolo[3,4-*b*]pyridine (35). To a mixture of **34** (600 mg, 1.40 mmol) and anisole (0.23 mL, 2.11 mmol), TFA (3 mL) was added and stirred at reflux for 5 h. After cooling to room temperature, the reaction mixture was concentrated *in vacuo*. The residue was purified by column chromatography (eluent, 0%–20% MeOH in EtOAc) to obtain 379 mg (88%) of **35** as a pale-yellow powder. UPLC-MS (ESI) *m/z*=308.4 [M+H]⁺, *t_R*=0.94 min. ¹H NMR (400 MHz, DMSO-*d*₆) δ 1.03 (d, *J*=6.6 Hz, 6H), 3.08 (spt, *J*=6.8 Hz, 1H), 3.83 (s, 3H), 7.20 (d, *J*=5.1 Hz, 1H), 7.70 (s, 1H), 7.78–7.82 (m, 1H), 7.93 (s, 1H), 8.09–8.14 (m, 1H), 8.56 (d, *J*=4.8 Hz, 1H), 13.65 (brs, 1H).

4-(3-Isopropyl-4-(4-(1-methyl-1*H*-pyrazol-4-yl)-1*H*-imidazol-1-yl)-1*H*-pyrazolo[3,4-*b*]pyridin-1-yl)benzonitrile (36a). The mixture of **35** (150 mg, 0.49 mmol), 4-fluorobenzonitrile (76.8 mg, 0.63 mmol), Cs₂CO₃ (207 mg, 0.63 mmol), and DMF (1.8 mL) was stirred at 50 °C for 30 min under nitrogen atmosphere. After cooling to room temperature, the reaction mixture was

diluted with EtOAc and water. The organic phase was washed with brine, dried over anhydrous MgSO_4 , and concentrated *in vacuo*. The residue was purified by column chromatography (eluent, 12%–100% EtOAc in hexane and 0%–20% MeOH in EtOAc) to obtain 162 mg (81%) of **36a** as a white powder. UPLC-MS (ESI) $m/z=409.1$ $[\text{M}+\text{H}]^+$, $t_R=1.68$ min. ^1H NMR (400 MHz, CDCl_3) δ 1.25 (d, $J=6.6$ Hz, 6H), 3.14 (spt, $J=6.8$ Hz, 1H), 3.98 (s, 3H), 7.20 (d, $J=4.9$ Hz, 1H), 7.34 (d, $J=1.2$ Hz, 1H), 7.76–7.86 (m, 5H), 8.63–8.67 (m, 2H), 8.71 (d, $J=4.9$ Hz, 1H).

4-(3-Isopropyl-4-(4-(1-methyl-1*H*-pyrazol-4-yl)-1*H*-imidazol-1-yl)-1*H*-pyrazolo[3,4-*b*]pyridin-1-yl)-2-(methylamino)benzonitrile (36b). The mixture of **35** (200 mg, 0.65 mmol), 4-iodo-2-(methylamino)benzonitrile (**S1**) (185 mg, 0.72 mmol), CuI (12.4 mg, 0.07 mmol), DMEDA (14 μL , 0.13 mmol), K_3PO_4 (290 mg, 1.37 mmol), and 1,4-dioxane (2.0 mL) was stirred at 110 °C for 24 h under nitrogen atmosphere. After cooling to room temperature, the reaction mixture was diluted with EtOAc and filtered through a pad of celite. The celite pad was washed with EtOAc and the filtrate was concentrated *in vacuo*. The residue was purified by column chromatography (eluent, 12%–100% EtOAc in hexane and 0%–20% MeOH in EtOAc) to obtain 103 mg (36%) of **36b** as a pale-yellow powder. UPLC-MS (ESI) $m/z=438.4$ $[\text{M}+\text{H}]^+$, $t_R=1.63$ min. ^1H NMR (400 MHz, CDCl_3) δ 1.24 (d, $J=6.6$ Hz, 6H), 3.06 (d, $J=5.1$ Hz, 3H), 3.08–3.18 (m, 1H), 3.97 (s, 3H), 4.77 (d, $J=5.1$ Hz, 1H), 7.16 (d, $J=4.8$ Hz, 1H), 7.32–7.35 (m, 1H), 7.53 (d, $J=8.4$ Hz, 1H), 7.78–7.86 (m, 5H), 8.68 (d, $J=4.8$ Hz, 1H).

4-(3-Isopropyl-4-(4-(1-methyl-1*H*-pyrazol-4-yl)-1*H*-imidazol-1-yl)-1*H*-pyrazolo[3,4-*b*]pyridin-1-yl)-3-nitrobenzonitrile (37). The mixture of **35** (200 mg, 0.65 mmol), 4-fluoro-3-nitrobenzonitrile (130 mg, 0.78 mmol), Cs_2CO_3 (276 mg, 0.85 mmol), and DMF (2.0 mL) was stirred at 80 °C for 14 h under nitrogen atmosphere. After cooling to room temperature, the reaction mixture was diluted with EtOAc and water. The organic phase was washed with brine,

dried over anhydrous MgSO_4 , and concentrated *in vacuo*. The residue was purified by column chromatography (eluents, 12%–100% EtOAc in hexane and 0%–20% MeOH in EtOAc) to obtain 205 mg (70%) of **37** as a brown powder. UPLC-MS (ESI) $m/z=454.8$ $[\text{M}+\text{H}]^+$, $t_R=1.56$ min. ^1H NMR (400 MHz, $\text{DMSO}-d_6$) δ 1.05 (d, $J=7.0$ Hz, 6H), 3.22 (spt, $J=6.8$ Hz, 1H), 3.86 (s, 3H), 7.52 (d, $J=5.1$ Hz, 1H), 7.72 (s, 1H), 7.91 (d, $J=1.5$ Hz, 1H), 7.96 (s, 1H), 8.22 (d, $J=1.5$ Hz, 1H), 8.34–8.41 (m, 2H), 8.72 (d, $J=4.8$ Hz, 1H), 8.75 (d, $J=1.8$ Hz, 1H).

3-Amino-4-(3-isopropyl-4-(4-(1-methyl-1H-pyrazol-4-yl)-1H-imidazol-1-yl)-1H-pyrazolo[3,4-*b*]pyridin-1-yl)benzonitrile (38). The mixture of **37** (200 mg, 0.44 mmol), Fe powder (246 mg, 4.41 mmol), NH_4Cl (236 mg, 4.41 mmol), THF (2.0 mL), MeOH (2.0 mL), and water (2.0 mL) was stirred at 80 °C for 4 h under nitrogen atmosphere. After cooling to room temperature, the reaction mixture was diluted with EtOAc and filtered through a pad of celite. The celite pad was washed with EtOAc, and the filtrate was dried over MgSO_4 and concentrated *in vacuo*. The residue was purified by column chromatography (eluents, 12%–100% EtOAc in hexane and 0%–20% MeOH in EtOAc) to obtain 72.2 mg (39%) of **38** as a pale-yellow powder. UPLC-MS (ESI) $m/z=424.3$ $[\text{M}+\text{H}]^+$, $t_R=1.38$ min. ^1H NMR (400 MHz, CDCl_3) δ 1.23 (d, $J=7.0$ Hz, 6H), 3.11–3.23 (m, 1H), 3.97 (s, 3H), 4.89 (brs, 2H), 7.17–7.21 (m, 3H), 7.35 (d, $J=1.1$ Hz, 1H), 7.77–7.86 (m, 4H), 8.66 (d, $J=5.1$ Hz, 1H).

4-(3-Isopropyl-4-(4-(1-methyl-1H-pyrazol-4-yl)-1H-imidazol-1-yl)-1H-pyrazolo[3,4-*b*]pyridin-1-yl)-3-(methylamino)benzonitrile (39). The mixture of **38** (58.9 mg, 0.14 mmol), $\text{Cu}(\text{OAc})_2$ (63.2 mg, 0.35 mmol), pyridine (39.4 μL , 0.49 mmol), and 1,4-dioxane (1.6 mL) was stirred at room temperature for 15 min under nitrogen atmosphere. To the reaction mixture, methylboronic acid (20.8 mg, 0.35 mmol) was added and stirred at 120 °C for 2 h. After cooling to room temperature, the reaction mixture was diluted with EtOAc and filtered through a pad of

celite. The celite pad was washed with EtOAc and concentrated *in vacuo*. The residue was purified by column chromatography (eluent, 12%–100% EtOAc in hexane and 0%–20% MeOH in EtOAc) to obtain 22.9 mg (38%) of **39** as a pale-yellow powder. UPLC-MS (ESI) $m/z=438.4$ $[M+H]^+$, $t_R=1.52$ min. 1H NMR (400 MHz, $CDCl_3$) δ 1.24 (d, $J=6.6$ Hz, 6H), 2.89 (d, $J=5.1$ Hz, 3H), 3.17 (spt, $J=6.8$ Hz, 1H), 3.97 (s, 3H), 5.68–5.73 (m, 1H), 7.06–7.07 (m, 1H), 7.13–7.18 (m, 2H), 7.35 (s, 1H), 7.73 (d, $J=8.1$ Hz, 1H), 7.78–7.82 (m, 3H), 8.65 (d, $J=5.1$ Hz, 1H).

Ancillary Information

Supporting Information

The Supporting Information is available free of charge on the ACS Publications website at DOI: <http://pubs.acs.org>.

Molecular formula strings and biological data (CSV)

The complete synthesis procedures and characterization of intermediates and test compounds whose procedures are not included in the main article, X-ray crystallography data and refinement statistics.

Accession Codes

The coordinates of the crystal structure of HSP90 in complex with compound **16d** (5ZR3) have been deposited in the Protein Data Bank. The authors will release the atomic coordinates and experimental data upon article publication.

Corresponding author information

*Phone: +81-29-865-4527. Fax: +81-29-865-2170. E-mail: takao-uno@taiho.co.jp

ORCID

Takao Uno: 0000-0002-3259-4603

Notes

The authors declare no competing financial interest. Author Contributions

Author Contributions

All the authors contributed to draft the manuscript. All authors have given approval to the final version of the manuscript.

Acknowledgments

We acknowledge Mr. Hirokazu Ohsawa for carrying out the HRMS analysis; Mr. Atsushi Hirano for measuring the LogD values and the solubility at pH 7.4; Mr. Kenjiro Ito for assistance in carrying out the *in vivo* efficacy study. We thank Dr. Teruhiro Utsugi, Dr. Kazuhiko Yonekura and Dr. Yoshikazu Iwasawa for their insightful discussion. We also thank all the departments at the Discovery and Preclinical Research Division of Taiho for the support they provided in this study.

Abbreviations used

SAR, Structure-activity relationship; HSR, heat shock response; MW, molecular weight; TPSA, topological polar surface area; ¹H NMR, proton nuclear magnetic resonance; UPLC-MS, ultra performance liquid chromatography-mass spectrometry; Pd(PPh₃)₄, tetrakis(triphenylphosphine)palladium (0); Na₂CO₃, sodium carbonate; DME, 1,2-dimethoxyethane; CuI, copper (I) iodide; DMEDA, *N,N'*-dimethylethylene diamine; Cs₂CO₃,

cesium carbonate; NaOH, sodium hydroxide; H₂O₂, hydrogen peroxide; DMSO, dimethyl sulfoxide; EtOH, ethanol; Pd(dppf)Cl₂.CH₂Cl₂, [1,1'-bis(diphenylphosphino)ferrocene]dichloropalladium (II); K₃PO₄, tripotassium phosphate; LDA, lithium diisopropylamide; THF, tetrahydrofuran; DIPA, diisopropylamine; *n*-BuLi, *n*-butyllithium; NaH, sodium hydride; DMF, *N,N*-dimethylformamide; DIPEA, *N,N*-diisopropylethylamine; CuO (II), copper (II) oxide; K₂CO₃, potassium carbonate; PMBCl, *p*-methoxybenzylchloride; Cu₂O, copper (I) oxide; PEG, polyethylene glycol; TFA, trifluoroacetic acid; NH₄Cl, ammonium chloride; Cu(OAc)₂, copper (II) acetate; CHCl₃, chloroform; MgSO₄, magnesium sulfate; MeOH, methanol; EtOAc, ethyl acetate; Na₂S₂O₃, sodium thiosulfate; Na₂SO₄, sodium sulfate; NaCl, sodium chloride.

References

- (1) Trepel, J.; Mollapour, M.; Giaccone, G.; Neckers, L. Targeting the dynamic HSP90 complex in cancer. *Nat Rev Cancer* **2010**, *10*, 537–549.
- (2) Whitesell, L.; Lindquist, S. L. HSP90 and the chaperoning of cancer. *Nat Rev Cancer* **2005**, *5*, 761–772.
- (3) Neckers, L.; Workman, P. Hsp90 molecular chaperone inhibitors: are we there yet? *Clin Cancer Res.* **2012**, *18*, 64–76.
- (4) Scaltriti, M.; Dawood, S.; Cortes, J. Molecular pathways: targeting hsp90—who benefits and who does not. *Clin Cancer Res.* **2012**, *18*, 4508–4513.
- (5) Ferrarini, M.; Heltai, S.; Zocchi, M. R.; Rugarli, C. Unusual expression and localization of heat-shock proteins in human tumor cells. *Int J Cancer* **1992**, *51*, 613–619.

- (6) Ciocca, D. R.; Calderwood S. K. Heat shock proteins in cancer: diagnostic, prognostic, predictive, and treatment implications. *Cell Stress Chaperones* **2005**, *10*, 86-103.
- (7) Kamal, A.; Thao, L.; Sensintaffar, J.; Zhang, L.; Boehm, M. F.; Fritz, L. C.; Burrows, F. J. A highaffinity conformation of Hsp90 confers tumour selectivity on Hsp90 inhibitors. *Nature* **2003**, *425*, 407–410.
- (8) Vilenchik, M.; Solit, D.; Basso, A.; Huezo, H.; Lucas, B.; He, H.; Rosen, N.; Spampinato, C.; Modrich, P.; Chiosis, G. Targeting wide-range oncogenic transformation via PU24FCI, a specific inhibitor of tumor Hsp90. *Chem Biol.* **2004**, *11*, 787–797.
- (9) Garcia-Carbonero, R.; Carnero, A.; Paz-Ares, L. Inhibition of HSP90 molecular chaperones: moving into the clinic. *Lancet Oncol.* **2013**, *14*, e358–e369.
- (10) Jhaveri, K.; Taldone, T.; Modi, S.; Chiosis, G. Advances in the clinical development of heat shock protein 90 (Hsp90) inhibitors in cancers. *Biochim Biophys Acta* **2012**, *1823*, 742–755.
- (11) Whitesell, L.; Mimnaugh, E. G.; De Costa, B.; Myers, C. E.; Neckers, L. M. Inhibition of heat shock protein Hsp90-pp60v-src heteroprotein complex formation by benzoquinone ansamycins: essential role for stress protein in oncogenic transformation. *Proc. Natl. Acad. Sci. U.S.A.* **1994**, *91*, 8324–8328.
- (12) Schulte, T. W.; Neckers, L. M. The benzoquinoneansamycin-17-allylamino-17-demethoxygeldanamycin binds to HSP90 and shares important biologic activities with geldanamycin. *Cancer Chemother. Pharmacol.* **1998**, *42*, 273– 279.

- (13) Kaur, G.; Belotti, D.; Burger, A. M.; Fisher-Nielson, K.; Borsotti, P.; Riccardi, E.; Thillainathan, J.; Hollingshead, M.; Sausville, E. A.; Giavazzi, R. Antiangiogenic properties of 17-(dimethylaminoethylamino)-17-demethoxygeldanamycin: an orally bioavailable heat shock protein 90 modulator. *Clin. Cancer Res.* **2004**, *10*, 4813– 4821.
- (14) Ge, J.; Normant, E.; Porter, J. R.; Ali, J. A.; Dembski, M. S.; Gao, Y.; Georges, A. T.; Grenier, L.; Pak, R. H.; Patterson, J.; Sydor, J. R.; Tibbitts, T. T.; Tong, J. K.; Adams, J.; Palombella, V. J. Design, synthesis, and biological evaluation of hydroquinone derivatives of 17-amino-17-demethoxygeldanamycin as potent, water-soluble inhibitors of Hsp90. *J. Med. Chem.* **2006**, *49*, 4606– 4615.
- (15) Sydor, J. R.; Normant, E.; Pien, C. S.; Porter, J. R.; Ge, J.; Grenier, L.; Pak, R. H.; Ali, J. A.; Dembski, M. S.; Hudak, J.; Patterson, J.; Penders, C.; Pink, M.; Read, M. A.; Sang, J.; Woodward, C.; Zhang, Y.; Grayzel, D. S.; Wright, J.; Barrett, J. A.; Palombella, V. J.; Adams, J.; Tong, J. K. Development of 17-allylamino-17-demethoxygeldanamycin hydroquinone hydrochloride (IPI-504), an anti-cancer agent directed against Hsp90. *Proc. Natl. Acad. Sci. U.S.A.* **2006**, *103*, 17408– 17413.
- (16) Samuni, Y.; Ishii, H.; Hyodo, F.; Samuni, U.; Krishna, M. C.; Goldstein, S.; Mitchell, J. B. Reactive oxygen species mediate hepatotoxicity induced by the Hsp90 inhibitor geldanamycin and its analogs. *Free Radic Biol Med* **2010**, *48*, 1559–1563.
- (17) Oh, W. K.; Galsky, M. D.; Stadler, W. M.; Srinivas, S.; Chu, F.; Bubley, G.; Goddard, J.; Dunbar, J.; Ross, R. W. Multicenter phase 2 trial of the Hsp-90 inhibitor, IPI-504 (retaspimycin hydrochloride), in patients with castration-resistant prostate cancer. *Urology*. **2011**, *78*, 626-630.

- (18) Kasibhatla, S. R.; Hong, K.; Biamonte, M. A.; Busch, D. J.; Karjian, P. L.; Sensintaffar, J. L.; Kamal, A.; Lough, R. E.; Brekken, J.; Lundgren, K.; Grecko, R.; Timony, G. A.; Ran, Y.; Mansfield, R.; Fritz, L. C.; Ulm, E.; Burrows, F. J.; Boehm, M. F. Rationally designed high-affinity 2-amino-6-halopurine heat shock protein 90 inhibitors that exhibit potent antitumor activity. *J. Med. Chem.* **2007**, *50*, 2767–2778.
- (19) Lundgren, K.; Zhang, H.; Brekken, J.; Huser, N.; Powell, R. E.; Timple, N.; Busch, D. J.; Neely, L.; Sensintaffar, J. L.; Yang, Y. C.; McKenzie, A.; Friedman, J.; Scannevin, R.; Kamal, A.; Hong, K.; Kasibhatla, S. R.; Boehm, M. F.; Burrows, F. J. BIIB021, an orally available, fully synthetic small-molecule inhibitor of the heat shock protein Hsp90. *Mol Cancer Ther* **2009**, *8*, 921–929.
- (20) Saif, M. W.; Takimoto, C.; Mita, M.; Banerji, U.; Lamanna, N.; Castro, J.; O'Brien, S.; Stogard, C.; Von Hoff, D. A phase 1, dose-escalation, pharmacokinetic and pharmacodynamic study of BIIB021 administered orally in patients with advanced solid tumors. *Clin Cancer Res.* **2014**, *20*, 445–455.
- (21) Renouf, D. J.; Velazquez-Martin, J. P.; Simpson, R.; Siu, L. L.; Bedard, P. L.; Ocular toxicity of targeted therapies. *J Clin Oncol.* **2012**, *30*, 3277–3286.
- (22) Brough, P. A.; Aherne, W.; Barril, X.; Borgognoni, J.; Boxall, K.; Cansfield, J. E.; Cheung, K. J.; Collins, I.; Davies, N. G. M.; Drysdale, M. J.; Dymock, B.; Eccles, S. A.; Finch, H.; Fink, A.; Hayes, A.; Howes, R.; Hubbard, R. E.; James, K.; Jordan, A. M.; Lockie, A.; Martins, V.; Massey, A.; Matthews, T. P.; McDonald, E.; Northfield, C. J.; Pearl, L. H.; Prodromou, C.; Ray, S.; Raynaud, F. I.; Roughley, S. D.; Sharp, S. Y.; Surgenor, A.; Walmsley, D. L.; Webb, P.; Wood, M.; Workman, P.; Wright, L. 4,5-Diarylisoazole Hsp90

chaperone inhibitors: potential therapeutic agents for the treatment of cancer. *J. Med. Chem.* **2008**, *51*, 196–218.

(23) Delmotte, P.; Delmotte-Plaque, J. A new antifungal substance of fungal origin. *Nature* **1953**, *171*, 344–345.

(24) Sessa, C.; Shapiro, G. I.; Bhalla, K. N.; Britten, C.; Jacks, K. S.; Mita, M.; Papadimitrakopoulou, V.; Pluard, T.; Samuel, T. A.; Akimov, M.; Quadts, C.; Fernandez-Ibarra, C.; Lu, H.; Bailey, S.; Chica, S.; Banerji, U. First-in-human phase I dose-escalation study of the HSP90 inhibitor AUY922 in patients with advanced solid tumors. *Clin Cancer Res.* **2013**, *19*, 3671–3680.

(25) Huang, K.H.; Veal, J. M.; Fadden, R. P.; Rice, J. W.; Eaves, J.; Strachan, J. P.; Barabasz, A.F.; Foley, B. E.; Barta, T. E.; Ma, W.; Silinski, M. A.; Hu, M.; Partridge, J. M.; Scott, A.; DuBois, L.G.; Freed, T.; Steed, P. M.; Ommen, A. J.; Smith, E. D.; Hughes, P. F.; Woodward, A. R.; Hanson, G. J.; McCall, W. S.; Markworth, C. J.; Hinkley, L.; Jenks, M.; Geng, L.; Lewis, M.; Otto, J.; Pronk, B.; Verleysen, K.; Hall, S. E. Discovery of novel 2-aminobenzamide inhibitors of heat shock protein 90 as potent, selective and orally active antitumor agents. *J. Med. Chem.* **2009**, *52*, 4288–4305.

(26) Rajan, A.; Kelly, R. J.; Trepel, J. B.; Kim, Y. S.; Alarcon, S. V.; Kummar, S.; Gutierrez, M.; Crandon, S.; Zein, W. M.; Jain, L.; Mannargudi, B.; Figg, W. D.; Houk, B. E.; Shnaidman, M.; Brega, N.; Giaccone, G. A phase I study of PF-04929113 (SNX-5422), an orally bioavailable heat shock protein 90 inhibitor, in patients with refractory solid tumor malignancies and lymphomas. *Clin Cancer Res.* **2011**, *17*, 6831–6839.

- (27) Powers, M. V.; Workman, P. Inhibitors of the heat shock response: biology and pharmacology *FEBS Lett.* **2007**, *581*, 3758–3769.
- (28) Eskew, J. D.; Sadikot, T.; Morales, P.; Duren, A.; Dunwiddie, I.; Swink, M.; Zhang, X.; Hembruff, S.; Donnelly, A.; Rajewski, R. A.; Blad, B.; Manjarrez, J. R.; Matts, R. L.; Holzbeierlein, J. M.; Vielhauer, G. A. Development and characterization of a novel C-terminal inhibitor of Hsp90 in androgen dependent and independent prostate cancer cells. *BMC Cancer*, **2011**, *11*, 468.
- (29) Koay, Y. C.; McConnell, J. R.; Wang, Y.; Kim, S. J.; Buckton, L. K.; Mansour, F.; McAlpine, S. R. Chemically accessible hsp90 inhibitor that does not induce a heat shock response. *ACS Med. Chem. Lett.* **2014**, *5*, 771-776.
- (30) Biamonte, M. A.; Van de Water, R.; Arndt, J. W.; Scannevin, R. H.; Perret, D.; Lee, W. C. Heat shock protein 90: inhibitors in clinical trials. *J. Med. Chem.* **2010**, *53*, 3-17.
- (31) Roughley, S. D.; Hubbard, R. E. How well can fragments explore accessed chemical space? A case study from heat shock protein 90. *J. Med. Chem.* **2011**, *54*, 3989-4005.
- (32) Barta, T. E.; Veal, J. M.; Rice, J. W.; Partridge, J. M.; Fadden, R. P.; Ma, W.; Jenks, M.; Geng, L.; Hanson, G. J.; Huang, K. H.; Barabasz, A. F.; Foley, B. E.; Otto, J.; Hall, S. E. Discovery of benzamide tetrahydro-4*H*-carbazol-4-ones as novel small molecule inhibitors of Hsp90. *Bioorg. Med. Chem. Lett.* **2008**, *18*, 3517-3521.
- (33) Fadden, P.; Huang, K.H.; Veal, J.M.; Steed, P. M.; Barabasz, A. F.; Foley, B.; Hu, M.; Partridge, J. M.; Rice, J.; Scott, A.; Dubois, L. G.; Freed, T. A.; Silinski, M. A.; Barta, T. E.; Hughes, P. F.; Ommen, A.; Ma, W.; Smith, E. D.; Spangenberg, A. W.; Eaves, J.; Hanson, G.

- J.; Hinkley, L.; Jenks, M.; Lewis, M.; Otto, J.; Pronk, G. J.; Verleysen, K.; Haystead, T. A.; Hall, S. E. Application of chemoproteomics to drug discovery: identification of a clinical candidate targeting Hsp90. *Chem. Biol.* **2010**, *17*, 686-694.
- (34) Thompson, F.; Mailliet, P.; Ruxer, J. M.; Goulaouic, H.; Vallée, F.; Minoux, H.; Pilorge, F.; Bertin, L.; Hourcade, S.; Mendez-perez, M.; Hamley, P. New fluorine derivatives, compositions containing the same and use thereof as inhibitors of the protein chaperone HSP 90. WO2008049994, May 2, 2008.
- (35) Mailliet, P.; Minoux, H.; Ruxer, J. M. Novel HSP90-inhibiting indole derivatives, compositions containing said derivatives, and use thereof. WO2011004132, January 13, 2011.
- (36) Nishimura, I.; Hirano, A.; Fukami, T. Improvement of the high-speed log*D* assay using an injection marker for the water plug aspiration/injection method. *J. Chromatogr. A* **2009**, *1216*, 2984-2988.
- (37) Yamashita, T.; Dohta, Y.; Nakamura, T.; Fukami, T. High-speed solubility screening assay using ultra-performance liquid chromatography/mass spectrometry in drug discovery. *J. Chromatogr. A* **2008**, *1182*, 72-76.
- (38) Kitade, M.; Okubo, S.; Yoshimura, C.; Yamashita, S.; Osiumi, H.; Uno, T.; Kawai, Y. Azabicyclo compound and salt thereof. WO2011004610, January 13, 2011.
- (39) Wright, L.; Barril, X.; Dymock, B.; Sheridan, L.; Surgenor, A.; Beswick, M.; Drysdale, M.; Collier, A.; Massey, A.; Davies, N.; Fink, A.; Fromont, C.; Aherne, W.; Boxall, K.; Sharp, S.; Workman, P.; Hubbard, R. E. Structure-activity relationships in purine-based inhibitor binding to HSP90 isoforms. *Chem Biol.* **2004**, *11*, 776-785.

- (40) Vallée, F.; Carrez, C.; Pilorge, F.; Dupuy, A.; Parent, A.; Bertin, L.; Thompson, F.; Ferrari, P.; Fassy, F.; Lamberton, A.; Thomas, A.; Arrebola, R.; Guerif, S.; Rohaut, A.; Certal, V.; Ruxer, J. M.; Gouyon, T.; Delorme, C.; Jouanen, A.; Dumas, J.; Grépin, C.; Combeau, C.; Goulaouic, H.; Dereu, N.; Mikol, V.; Mailliet, P.; Minoux, H. Tricyclic series of heat shock protein 90 (Hsp90) inhibitors part I: Discovery of tricyclic imidazo[4,5-*c*]pyridines as potent inhibitors of the Hsp90 molecular chaperone. *J. Med. Chem.* **2011**, *54*, 7206-7219.
- (41) Ohkubo, S.; Kodama, Y.; Muraoka, H.; Hitotsumachi, H.; Yoshimura, C.; Kitade, M.; Hashimoto, A.; Ito, K.; Gomori, A.; Takahashi, K.; Shibata, Y.; Kanoh, A.; Yonekura, K. TAS-116, a highly selective inhibitor of heat shock protein 90 α and β , demonstrates potent antitumor activity and minimal ocular toxicity in preclinical models. *Mol. Cancer. Ther.* **2015**, *14*, 14-22.
- (42) Howes, R.; Barril, X.; Dymock, B. W.; Grant, K.; Northfield, C. J.; Robertson, A. G.; Surgenor, A.; Wayne, J.; Wright, L.; James, K.; Matthews, T.; Cheung, K. M.; McDonald, E.; Workman, P.; Drysdale, M. J. A fluorescence polarization assay for inhibitors of Hsp90. *Anal Biochem* **2006**, *350*, 202–213.
- (43) Lea, W. A.; Simeonov, A. fluorescence polarization assays in small molecule screening. *Expert Opin Drug Discov* **2011**, *6*, 17–32.
- (44) Suzuki, R.; Hideshima, T.; Mimura, N.; Minami, J.; Ohguchi, H.; Kikuchi, S.; Yoshida, Y.; Gorgun, G.; Cirstea, D.; Cottini, F.; Jakubikova, J.; Tai, Y. T.; Chauhan, D.; Richardson, P. G.; Munshi, N. C.; Utsugi, T.; Anderson, K. C. Anti-tumor activities of selective

- HSP90 α/β inhibitor, TAS-116, in combination with bortezomib in multiple myeloma. *Leukemia*, **2015**, 29, 510-514.
- (45) Pao, W.; Miller, V. A.; Politi, K. A.; Riely, G. J.; Somwar, R.; Zakowski, M. F.; Kris, M. G.; Varmus, H. Acquired resistance of lung adenocarcinomas to gefitinib or erlotinib is associated with a second mutation in the EGFR kinase domain. *PLoS Med* **2005**, 2, e73.
- (46) Miyaura, N.; Suzuki, A. Palladium-catalyzed cross-coupling reactions of organoboron compounds. *Chem. Rev.* **1995**, 95, 2457-2483.
- (47) Antilla, J. C.; Klapars, A.; Buchwald, S. L. The copper-catalyzed *N*-arylation of indoles. *J. Am. Chem. Soc.* **2002**, 124, 11684-11688.
- (48) Antilla, J. C.; Baskin, J. M.; Barder, T. E.; Buchwald, S. L. Copper-diamine-catalyzed *N*-arylation of pyrroles, pyrazoles, indazoles, imidazoles, and triazoles. *J. Org. Chem.* **2004**, 69, 5578-5587.
- (49) Katritzky, A. R.; Pilarski, B.; Urogdi, L. Efficient Conversion of nitriles to amides with basic hydrogen peroxide in dimethyl sulfoxide. *Synthesis* **1989**, 949-950.
- (50) Sawaki, Y.; Ogata, Y. Mechanism of the reaction of nitriles with alkaline hydrogen peroxide. reactivity of peroxy-carboximidic acid and application to superoxide ion reaction. *Bull. Chem. Soc. Jpn.* **1981**, 54, 793– 799.
- (51) Hasegawa, T.; Kawanaka, Y.; Kasamatsu, E.; Ohta, C.; Nakabayashi, K.; Okamoto, M.; Hamano, M.; Takahashi, K.; Ohuchida, S.; Hamada, Y. A New process for synthesis of the astrocyte activation suppressor, ONO-2506. *Org. Process Res. Dev.* **2005**, 9, 774–781.

- (52) Schnürch, M.; Spina, M.; Khan, A. F.; Mihovilovic, M. D.; Stanetty, P. Halogen dance reactions—A review. *Chem. Soc. Rev.* **2007**, *36*, 1046-1057.
- (53) Kantam, M. L.; Yadav, J.; Laha, S.; Sreedhar, B.; Jha, S. *N*-arylation of heterocycles with activated chloro- and fluoroarenes using nanocrystalline copper(II) oxide. *Adv. Synth. Catal.* **2007**, *349*, 1938-1942.
- (54) Altman, R. A.; Koval, E. D.; Buchwald, S. L. Copper-catalyzed *N*-arylation of imidazoles and benzimidazoles. *J. Org. Chem.* **2007**, *72*, 6190-6199.
- (55) Boger, D. L.; Fink, B. E.; Hedrick, M. P. Total synthesis of distamycin A and 2640 analogues: A solution-phase combinatorial approach to the discovery of new, bioactive DNA binding agents and development of a rapid, high-throughput screen for determining relative DNA binding affinity or DNA binding sequence selectivity. *J. Am. Chem. Soc.* **2000**, *122*, 6382-6394.
- (56) Ramadas, K.; Srinivasan, N. Iron-ammonium chloride—A convenient and inexpensive reductant. *Synth. Commun.* **1992**, *22*, 3189-3195.
- (57) González, I.; Mosquera, J.; Guerrero, C.; Rodríguez, R.; Cruces, J. Selective monomethylation of anilines by Cu(OAc)₂-promoted cross-coupling with MeB(OH)₂. *Org. Lett.* **2009**, *11*, 1677-1680.
- (58) Kurokawa, Y.; Doi, T.; Sawaki, A.; Komatsu, Y.; Ozaka, M.; Takahashi, T.; Naito, Y.; Okubo, S.; Nishida, T. Phase II study of TAS-116, an oral inhibitor of heat shock protein 90 (HSP90), in metastatic or unresectable gastrointestinal stromal tumor refractory to imatinib, sunitinib and regorafenib. *Annals of Oncology* **2017**, *28* (suppl_5), 522-523.

- (59) Battye, T.G.; Kontogiannis, L.; Johnson, O.; Powell, H.R.; & Leslie, A.G. iMOSFLM: a new graphical interface for diffraction-image processing with MOSFLM. *Acta. Crystallogr. D Biol. Crystallogr.* **2011**, *67*, 271-281.
- (60) Collaborative Computational Project No. 4. The CCP4 suite: programs for protein crystallography. *Acta Crystallogr.* **1994**, *D50*, 760-763.
- (61) Vagin, A; Teplyakov, A. MOLREP: an automated program for molecular replacement. *J Appl Crystallogr* **1997**, *30*, 1022-1025.
- (62) Murshudov, G.N.; Vagin A.A.; Dodson, E.J. Refinement of macromolecular structures by the maximum-likelihood method. *Acta Crystallogr.* **1997**, *D53*, 240-255.
- (63) Emsley, P.; Lohkamp, B.; Scott, W. G.; Cowtan, K. Features and development of Coot. *Acta. Crystallogr. D Biol. Crystallogr.* **2010**, *66*, 486-501.

Table of Contents Graphic

